P. Kamphuis

September 2003

The formation of population III stars in the presence of a radiation field

Supervisor: Dr. M. Spaans

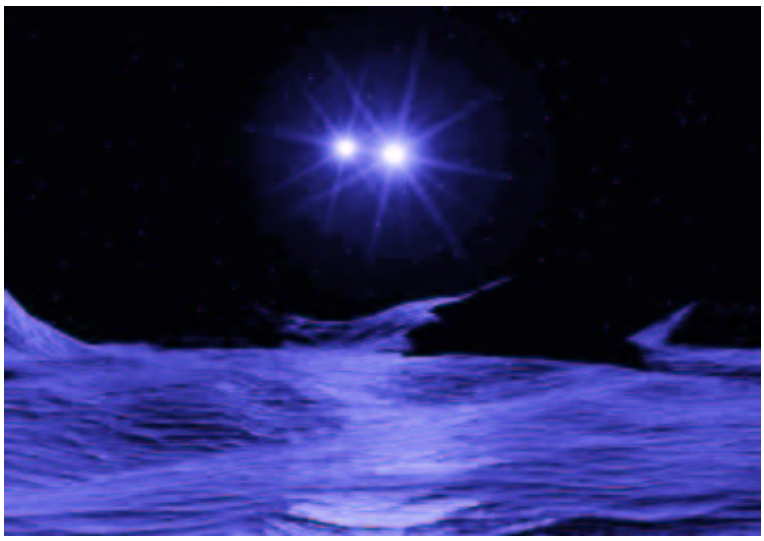

"The kids better buy my rookie card now
Cause after this stuff the price ain't comin' down"
- Mos Def

Abstract

Feedback is one of the most important problems in reionization. This paper explores the feedback of UV radiation on the H_2 in a proto-stellar gas cloud. The fate of H_2 in UV radiation fields is one of the biggest feedback problems because H_2 is the only coolant in the primordial gas below 10,000 K. Because of this H_2 determines the collapse of gas clouds during the reionization epoch. A simulation is done where a proto-stellar cloud without metals is subjected to a population III radiation field, and its density of H_2 is examined after irradiation. It is found that the very first stars provide a negative feedback to stars forming later. And thus stretch the epoch of reionization. It is found that, without considering fragmentation, the population III stars form as isolated objects in regions with a radius of 10 ± 2 pc.

Contents

1 Introduction and Outline

This paper is meant to provide some more insight into the feedback problems involved with the formation of Population III (Pop III) stars. In reionization, feedback is an important problem. Especially with the new results of WMAP which imply reionization has started as early as redshift seventeen. The possible detection of a Gunn-Peterson trough in a quasar at z=6.28, Becker et al. (2001), makes matters even worse. These two independent observations would imply that reionization has started at a redshift of z$\sim$17 but the universe was not completely ionized until a redshift of z$\sim$6. This provides serious problems to theorists and it indicates that reionization is a complex problem, Hui & Haiman (2003). Feedback could be a big part of the solution to this problem. Feedback could quench or speed up second generation star formation. Therefore, feedback is one of the key elements in the determination of the length of the reionization epoch. During the epoch of reionization many different forms of feedback are expected. For instance, the influence of an UV-background on gas clouds, the influence of an X-ray background on specific molecules in a gas cloud, the effect of supernovae of the first stars, contamination of the Inter Galactic Matter (IGM) and many other forms. This is all very important because pop III stars are assumed to be the building blocks of galaxies. Here lie the initial conditions for galaxy formation and evolution. If for instance due to feedback it would be impossible to form more than one pop III star or only very heavy stars which collapse into black holes without depositing metals in the IGM this could provide serious problems for the contamination of the IGM with metals in time, see Bertoldi et al. (2003). There are also theories that pop III provide the seeds for the massive black holes found in almost every galaxy. All of these problems and theories make the reionization epoch a very interesting time in our universe. And to solve these problems gives us the possibility to differentiate between several cosmological models and put better constraints on them. So although reionization happened a long time ago it can still tell us much about the present universe because it contains several of the initial conditions of the structures we see today and it can put constraints on others.

This paper investigates the influence of the radiation of a pop III star on a proto-stellar gas cloud in its vicinity. The study concentrates on the effects of the radiation on the molecular hydrogen molecules in the cloud. The H_2 molecules determine the cooling rate in the cloud which in turn determines the dynamics of its collapse. This is due to the fact that in a primordial gas there are no heavy elements and thus H_2 is the only molecule which is able to cool at temperatures below 10,000 K. Since H_2 is so important in pop III star formation, the dissociation or formation of this molecule is crucial for feedback effects. To determine if there is a positive or a negative feedback from radiation by the first pop III stars an IDL code, which uses analytical formulas to calculate the amount of molecular hydrogen in the cloud after it has been radiated upon for 9 million years by a pop III star, is written. The cloud used as a proto-stellar gas cloud is based on simulations done by Abel et al. (2002). Due to computational limitations only the inner core of 0.5 pc is considered. In the simulation twenty, different, radiation fields are used. These radiation fields resemble twenty pop III stars as they are believed to radiate according to present theory. Ten are temperature selected, in the range 20,000- 110,000 K, and ten are mass selected, in the range 5-250 $M_\odot$, to assure a wide and realistic range in mass and temperature. Also, 6 different distances (3-100 pc) from the cloud are considered. To determine the effect of feedback on the gas cloud we need a criterium for gravitational collapse. This criterium can be found in the different timescales that govern the cloud. The most important timescales, freefall time and cooling time, are discussed. The criterium that is used for gravitational instability is the minimum amount of molecular hydrogen necessary to radiate away the increase in binding energy between the steps given in Abel et al. (2002), i.e the cooling time. As it turns out these simulations already are around this minimum and so this shows again that collapse is governed by cooling and the fate of the H_2 is very important. Basically, if a reasonable fraction of the molecular hydrogen is destroyed no collapse will follow.

2 H_2 Dissociation

In HI regions we can assume that all radiation with energies above 13.6 eV is completely absorbed. This provides a problem for the dissociation of molecular hydrogen because the molecular photo-dissociation begins at 14.7 eV and its photo-ionization continuum starts at 15.4 eV. So on first hand it would look like there is negligible photo-dissociation of molecular hydrogen. But there are other mechanisms for the destruction of molecular hydrogen. These other mechanisms can be summed up by two equations:

$$\mathrm{H_2(X^1\Sigma_g^+, v=0)} \xrightarrow[\text{absorption at } \sim 1000\ \mathring{A}]{\text{rate } \beta} \mathrm{H_2(B^1\Sigma_u^+, v=v')} \rightarrow \mathrm{H_2(X, v=v'')} \tag{1}$$

$$\mathrm{H_2(X, v=v'')} \xrightarrow[\text{absorption at } \sim 1000\ \mathring{A}]{} \begin{cases} \mathrm{H_2^+ + e} \\ H + H \end{cases} \tag{2}$$

Where $X^1\Sigma_g^+$ is the ground state, $B^1\Sigma_u^+$ is the excited state in the Lyman band, v is the excitation level. The molecule is dissociated when the Lyman band emission $B \rightarrow X$ leaves the molecule in the vibrational continuum of the ground state. This happens when in equation (1) $v'' > 14$. If $2 < v'' \leq 14$ then photo-ionization and photo-dissociation is possible with photons of energies lower then 13.6 eV. This is indicated in equation (2). Equations for the $C^1\Pi_u$ state in the C-X Werner bands are the same, e.g. Stecher & Williams (1967). These bands lie between 900 and 1100 Å. Now the chance that an excited molecule will fall back to the vibrational continuum is somewhere around 15 %. For the other 85 % the electron will fall back to an excited vibration-rotation level of the ground state and produce a photon. This process is called H_2 fluorescence. These excited states decay by the electric quadruple transitions in the infrared on timescales of 10^6 s, see Black & Dalgarno (1976). Typically around wavelengths of 1-6 μm, c.f. Black & van Dishoeck (1987). It is also through this fluorescence that molecular hydrogen molecules are such good coolants compared to neutral hydrogen. To approximate the H_2-dissociation rate in a hydrogen cloud the following formula is used, de Jong et al. (1980):

$$R = p \frac{I_\nu d\Omega}{h\nu} \frac{\pi e^2}{m_e c} f n_L \beta(\tau) \qquad s^{-1} \tag{3}$$

Where p is the probability that molecules in an excited state decay into the vibrational continuum. I_ν is the intensity of the star near 1000 Å. $d\Omega$ is the solid angle of the star as seen from the cloud :

$$d\Omega = \frac{\Delta a}{D^2} \tag{4}$$

Zeilik et al. (1992). Here D is the distance from the cloud to the star and Δa is the surface area of the star. In our case, assuming a spherical star, $\Delta a = \pi R^2$ with R the radius of the star. f is the oscillator strength of a single Lyman line and n_L is the number of Lyman lines. $\beta(\tau)$ is the probability that photons penetrate to optical depth τ in the cloud. Notice that in equation (3) the usual exponential factor that takes account of attenuation by dust grains in the cloud is left out. This is because we assume there is no dust present in Pop III proto-stellar clouds. Also, the mean interstellar radiation density (u_ν multiplied by the speed of light) is replaced by the intensity multiplied by the solid angle. Photo-dissociation is limited to absorption of photons in the Lyman band ($X^1\Sigma_g^+ - B^1\Sigma_u^+$) and all the H_2 molecules are assumed to be in the electronic ground state ($X^1\Sigma_g^+$). From the above statements it is clear that the formula is only an approximation. The values used in this paper for equation (3) are listed in table (1). All other constants have their usual values. For the intensity (I_ν) a black body spectrum is used. For $\beta(\tau)$ the following formula is used:

$$\beta(\tau) = \left\{ \frac{1}{\tau[\ln(\tau/\sqrt{\pi})]^{\frac{1}{2}}} + \left(\frac{a}{\tau}\right)^{\frac{1}{2}} \right\} \mathrm{erfc} \left[\left(\frac{\tau a}{\pi v_1^2} \right)^{\frac{1}{2}} \right] \tag{5}$$

with

$$a = \frac{\gamma c}{4\pi\nu\delta V_D} \qquad \text{and} \qquad v_1 = \frac{\Delta\lambda_1 c}{\lambda \delta V_D} \tag{6}$$

p	0.15
f	4.6×10^{-3}
n_L	60

Table 1: Dissociation constants

At 1000 Å, a reciprocal lifetime of the upper state (γ) of 1.16×10^9 s, and an average separation of Lyman lines ($\Delta\lambda_1$) of 1.6 Å is assumed. This gives:

$$a = \frac{923.0987}{\delta V_D} \quad \text{and} \quad v_1 = \frac{5 \times 10^7}{\delta V_D} \tag{7}$$

Where a Gaussian turbulent velocity field is adopted for the cloud. δV_D is the velocity width of the turbulence which in these calculations was set to 1 km/s. τ is given by

$$\tau = \frac{\pi e^2}{mc} \frac{fc}{\delta V_D \nu} N(\mathrm{H_2}) = 1.2 \times 10^{-9} \frac{N(\mathrm{H_2})}{\delta V_D} \tag{8}$$

With $N(\mathrm{H_2})$ the column density of molecular hydrogen. Equation (5) has some problems at the edge where $\tau < \sqrt{\pi}$. In these cases the natural logarithm becomes negative and thus we try to take a negative square-root. Also when $\tau \sim \sqrt{\pi}$ still $\beta > 1$ but β can never be greater then 1 because without any extinction $\beta = 1$, de Jong et al. (1980). This is why in the simulations when $\tau < \sqrt{\pi}$ or $\beta > 1$, β is set to 1. Just behind the edge where β is set to 1 the simulations are a very poor approximation. To give an impression of the function β figure (1) is included. In figure (1) we show β for turbulent velocities 1, 3, 5, 7, 10 and 20 km/s (bottom to top) the rest of the values are as mentioned previously. The radius of the cloud is given in cm, where 0 is the center of the cloud. The y-axis is on a logarithmic scale because at the edge β shows a very fast decline into the cloud. The effects this has on the dissociation are discussed further on. In the figure we can see that increasing the turbulent velocity in the cloud diminishes the shielding, but this is not a big effect so errors in the turbulent velocity width are not significant. Finally note that the normal dissociation energy of $\mathrm{H_2}$ is 4.48 eV but transitions at this energy are strongly forbidden. This is because the molecule is homo-nuclear and without a dipole moment.

3 $\mathrm{H_2}$ formation

In HI regions $\mathrm{H_2}$ can as well be formed. In the absence of dust there are only three routes for this process, $\mathrm{H^-}$, $\mathrm{H_2^+}$ and three body formation. These three routes will be treated explicitly in this section.

3.1 $\mathrm{H^-}$ route

The $\mathrm{H^-}$ route is the recombination of H atoms with $\mathrm{H^-}$ ions.

$$\mathrm{H} + \mathrm{e^-} \rightarrow \mathrm{H^-} + h\nu, \tag{9}$$

$$\mathrm{H} + \mathrm{H^-} \rightarrow \mathrm{H_2} + \mathrm{e^-} \tag{10}$$

Notice that the $\mathrm{H^-}$ ion only acts as a catalyst, the electron which is set free in the end can form $\mathrm{H^-}$ again. So even with a low electron abundance, in time, a reasonable amount of $\mathrm{H_2}$ is formed, provided there is no dissociation. The formation rate can be calculated as follows, Cazaux & Spaans (2003):

$$R_f = k_1 n_H^2 \xi_e \quad cm^{-3} s^{-1} \tag{11}$$

Where $k_1 = 1.83 \times 10^{-18} T_g^{0.8779} \quad cm^3 s^{-1}$ with T_g the gas temperature and n_H the density of all hydrogen species. The electron fraction ξ_e can be obtained from:

$$\xi_e = 0.07 T_g^{0.42} \sqrt{\frac{J_{21}}{n_H}} \tag{12}$$

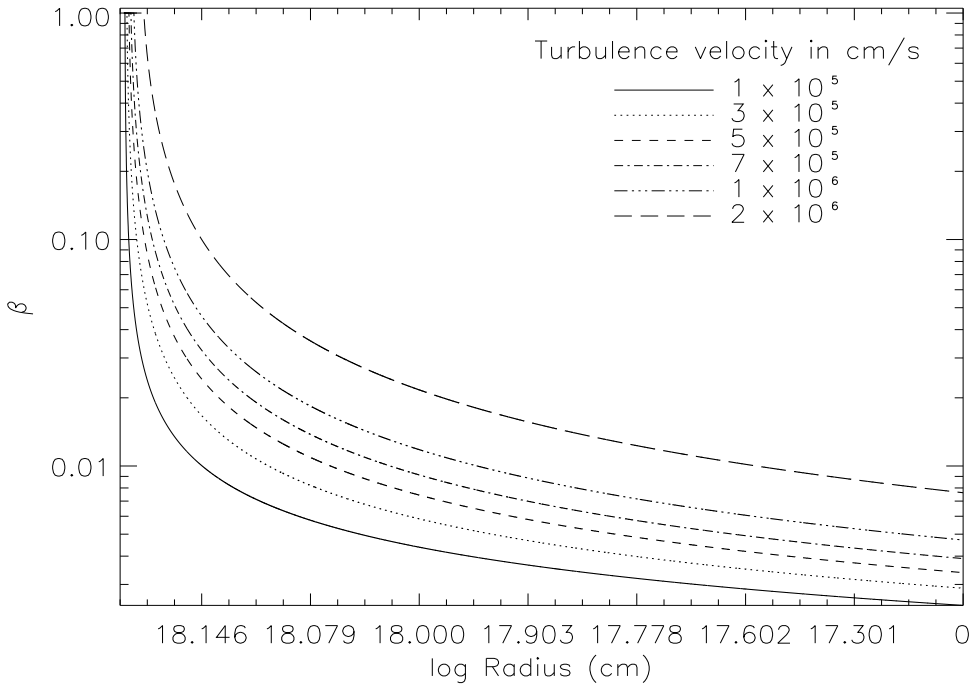

Figure 1: Impression of β for different turbulent velocities with from bottom to top, δV_D= 1, 3, 5, 7, 10, 20 km/s.

J_{21} can be calculated with the formula:

$$J_{21} = 8.18 \times 10^{-13} I_{21} \tau_f^{-\frac{8}{3}} \quad s^{-1} \tag{13}$$

with

$$I_{21} = \frac{I(1000\text{Å})d\Omega}{2\pi \times 10^{-21}} \quad erg\ s^{-1} sr^{-1} \tag{14}$$

Where I(1000 Å) is the intensity at 1000 Å of a black body with a temperature equal to the effective temperature of the star which is shining onto the cloud. τ_f is

$$\tau_f = 6.3 \times 10^{-18} \mathrm{N_{col}} \tag{15}$$

Where $\mathrm{N_{col}}$ is the neutral hydrogen column density. τ_f differs from the optical depth used in dissociation, this is because for the formation of H_2 the electron abundance is important and the electrons come from ionized hydrogen. So here the radiation absorbed by neutral hydrogen is taken out for forming molecular hydrogen. This is not so for dissociation where only radiation absorbed by molecular hydrogen affects the dissociation rate. Hence the different optical depths for formation and dissociation. $d\Omega$ is the same as in formula (4). Figure (2) is included to show the dependence of the electron abundance on gas temperature. For gas temperatures, from top to bottom, 100, 200, 300, 400, 500, 600 and 700 K. We see a decline into the cloud due to the shielding effect of neutral hydrogen. 0 indicates the core cloud center.

3.2 Three body formation

At high densities ($\mathrm{n_H} \geq 10^8$ cm^{-3}) molecular hydrogen can be formed also through three body interactions. Basically:

$$\mathrm{H + H + H \rightarrow H_2 + H} \tag{16}$$

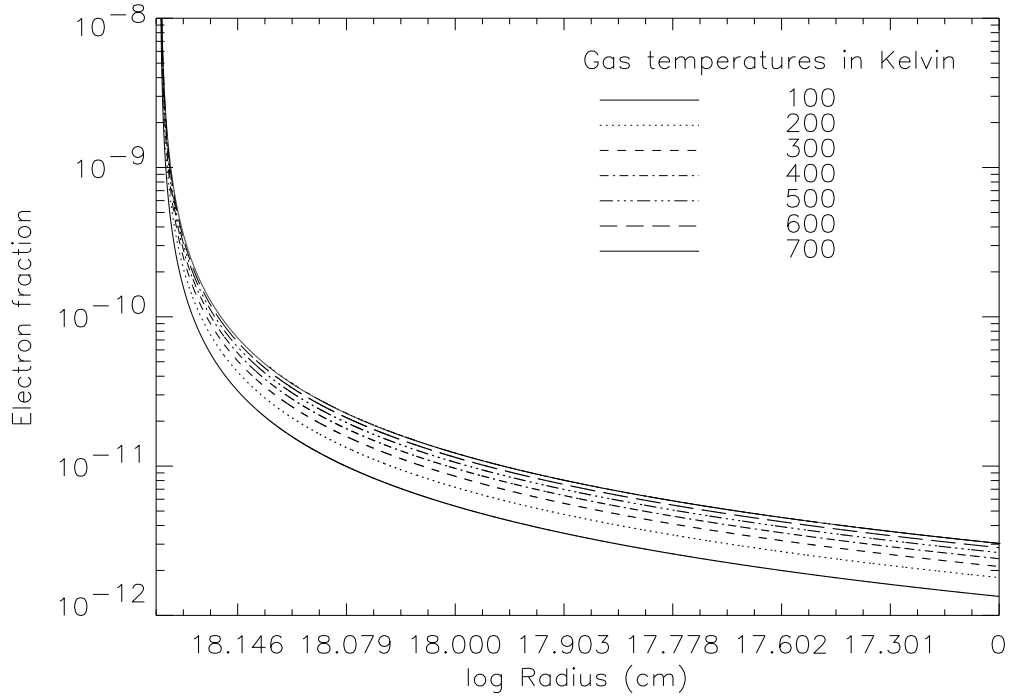

Figure 2: Impression of ξ for different gas temperatures with, from bottom to top, T_g= 100, 200, 300, 400, 500, 600 and 700 K for all temperatures n(H)=1×10^3.

$$H + H + H_2 \rightarrow H_2 + H_2 \tag{17}$$

At these densities this reaction is so efficient that all the neutral hydrogen will be converted into H_2, Palla et al. (1983). To check this we can take a look at the rate constants of the reactions. For

$$H + H + H \underset{k_2}{\overset{k_1}{\rightleftharpoons}} H_2 + H \tag{18}$$

we have

$$k_1 = 5.5 \times 10^{-29} T_g^{-1} \quad \mathrm{cm^3 s^{-1}} \tag{19}$$

With T_g the gas temperature, and

$$k_2 = 6.5 \times 10^{-7} T_g^{-\frac{1}{2}} \exp\left(-\frac{52.000}{T_g}\right) \times \left[1 - \exp\left(-\frac{6000}{T_g}\right)\right] \quad \mathrm{cm^3 s^{-1}} \tag{20}$$

Palla et al. (1983). If we compare k_1 and k_2 we can see that for temperatures $T_g < 800$K the leftward reaction is negligible. So the balance for this reaction lies to almost 100% H_2. Thus, in the absence of a radiation field the formed H_2 will not be dissociated. For

$$H + H + H_2 \underset{k_4}{\overset{k_3}{\rightleftharpoons}} H_2 + H_2 \tag{21}$$

We have

$$k_3 = \frac{1}{8} k_1 \quad \text{and} \quad k_4 = \frac{1}{8} k_2 \tag{22}$$

So it is the same as for equations (19, 20), only this route is less efficient.

3.3 H_2^+ Route

The H_2^+ route is

$$H^+ + H \rightarrow H_2^+ + h\nu \tag{23}$$

$$H_2^+ + H \rightarrow H_2 + H^+ \tag{24}$$

This way of forming molecular hydrogen is very inefficient and is not included in our simulations. Although this route may become important at very high redshift ($z > 500$) where the H^- is destroyed by the cosmic microwave background radiation field.

4 Radiation sources

As a radiation source we take a single pop III star which is shining onto the cloud. In the simulations we have taken 20 different stars of which the properties are listed in table (2). We have taken a series of stars so that they span the whole range of possible masses, and another set of stars so that they span a range of plausible effective temperatures. The other

Temperature(K)	Mass($M_\odot$)	Radius ($R_\odot$)	Lifetime (years)
temperature selected			
2×10^4	3	1.12	1.11×10^9
3×10^4	5	1.40	4.00×10^8
75×10^3	25	2.9	1.60×10^7
8×10^4	34	3.4	8.65×10^6
85×10^3	40	3.6	6.25×10^6
9×10^4	60	4.3	2.78×10^6
95×10^3	70	4.7	2.04×10^6
1×10^5	141	6.4	5.03×10^5
105×10^3	218	7.8	2.10×10^5
11×10^4	401	10.37	6.22×10^4
mass selected			
3×10^4	5	1.40	4.00×10^8
72443	20	2.65	2.50×10^7
86099	50	4.03	4.00×10^6
95499	75	4.84	1.78×10^6
97948	100	5.52	1.00×10^6
99390	125	6.11	6.40×10^5
100818	150	6.63	4.44×10^5
102435	175	7.12	3.26×10^5
104712	200	7.56	2.50×10^5
105715	250	8.37	1.60×10^5

Table 2: Values for the radiation sources used.

values are then calculated.
If we choose a temperature we can estimate the related masses from fig. 1 in Tumlinson & Shull (2000) for masses below a 100 $M_\odot$ and from fig. 1 of Bromm et al. (2001) for masses higher then 100 $M_\odot$. With these values we can see how much the analytical formula of Bromm et al. (2001) is off in metallicity. This formula is:

$$T_{eff} \simeq (1.1 \times 10^5) \left(\frac{Z}{10^{-9}}\right)^{-0.05} \left(\frac{M}{100 M_\odot}\right)^{0.025} \quad K. \tag{25}$$

The metallicities we get in this way are used to calculate the effective temperatures of certain masses.
With the formula

$$M \simeq (370 M_\odot) \left(\frac{Z}{10^{-9}}\right)^{-0.2} \left(\frac{R}{10 R_\odot}\right)^{2.2} \quad M_\odot \tag{26}$$

we can then calculate the radii of the stars. This formula is quite exact and even goes down to very low masses where it still seems to be in good agreement with the values published

by Chabrier & Baraffe (1997). So for this formula we can assume metallicities of $Z = 10^{-9}$. Lifetimes are calculated with the formula

$$t_* = \left(\frac{M_*}{M_\odot}\right)^{-2} t_\odot. \tag{27}$$

This formula is actually for normal stars. But the assumption is that the increase in error by the difference with pop III stars is relatively small. See also section 6.1.

5 Cloud structure

The structure of the gas cloud is based on calculations of a collapsing primordial gas cloud, Abel et al. (2002). This cloud is a collapsing sphere so there is no dynamical equilibrium established.

For the simulations only the inner 0.5 pc is considered. In the simulations the cloud is considered in three different stages. First the cloud is assumed to be as calculated at z =19 (purple solid line in figure (3)). Second a cloud is considered as calculated at the second step, which is 9 million years later (red dotted line). Last the average of the two steps is considered (see section (7)). At the first (second,average) step the cloud has a constant density of $n_H = 10^3\ cm^{-3}$ $(10^6, 5 \times 10^5)$ and a constant temperature of $T_g = 200\ K$ $(250, 225)$. For the starting conditions of the cloud we assume that there is only atomic and molecular hydrogen. The fraction of molecular hydrogen in the cloud is $f(n_{H_2}) = 10^{-3}$. As seen in figure (3) the cloud exhibits no gradients of any kind in the core considered here. H_2 cooling is important to get rid of radiation pressure which can stop the collapse. Now to know if the destruction of H_2 is enough to stop the collapse we have to look at timescales. The time it takes for the cloud to collapse will again come from Abel et al. (2002), other timescales will be treated below.

6 Timescales

If we want to know whether the H_2 is destroyed before the cloud has collapsed, we have to set a timescale. For instance, H_2 destruction could be so slow, due to absorption of radiation or the distance to the source of radiation, that the star will die before reasonable amounts of H_2 are destroyed. Or it could be that the cloud is already collapsing at such a speed that it has fully collapsed before a reasonable amount of H_2 is destroyed. So relevant timescales are, lifetime of the radiating star, freefall time of the cloud and the cooling timescale.

6.1 Lifetime of the star

The lifetime of the star is calculated in equation (27), but this is a formula for normal stars. Now to get a reasonable error we have to derive this formula and see where the differences between pop I/II and pop III come into the equation and how big these differences are.
Equation 27 is derived by the simple assumption that the lifetime of a star is the amount of energy it contains (the mass) divided by the amount of energy it radiates (the luminosity). So in mathematical form this is:

$$\frac{\mathrm{t_*}}{\mathrm{t_\odot}} = \frac{\mathrm{M_*}}{\mathrm{M_\odot}} / \frac{\mathrm{L_*}}{\mathrm{L_\odot}} \tag{28}$$

Now to get equation (27) a luminosity-mass relation is needed. This relation is calculated to be

$$\frac{\mathrm{L_*}}{\mathrm{L_\odot}} = \left(\frac{\mathrm{M_*}}{\mathrm{M_\odot}}\right)^{\alpha} \tag{29}$$

Where α is ~ 4 for normal stars and ~ 3 for massive stars. Now pop III stars do not differ from pop I/II stars in their mass-luminosity relation, Bromm et al. (2001). So, assuming

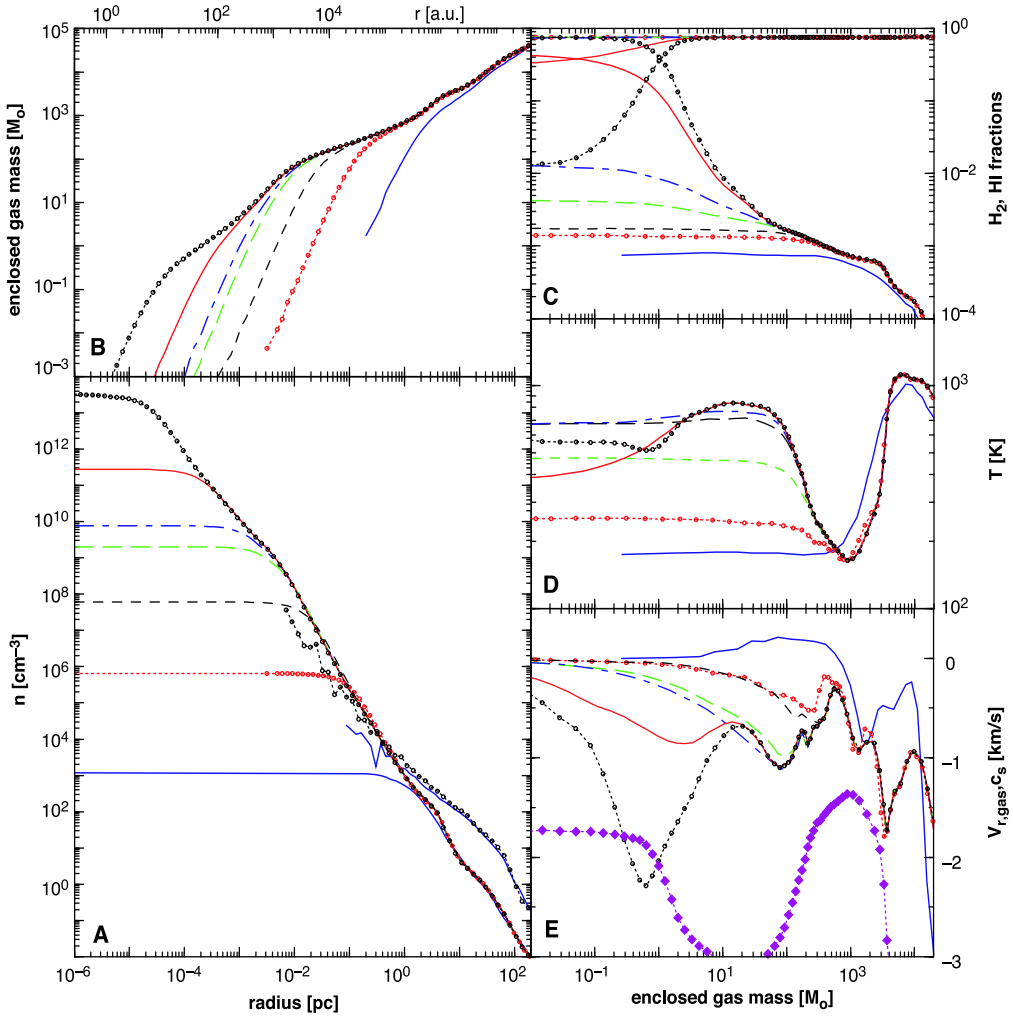

Figure 3: Figure from Abel et al. (2002), with (A) Evolution of the particle number density in cm^{-3} as a function of radius at redshift 19 (purple solid line) 9 million years later (red dotted lines with circles), 300,000 years later (black dashed line), 30,000 years later (green long-dashed line), 3000 years later (purple dot-dashed line), 1500 years later (red solid line), and 200 years later (black dotted line with circles) at z = 18.181164. The two lines between 10^{-2} and 200 pc give the DM mass density in GeV cm^{-3} at z = 19 and the final time, respectively.(B) Enclosed gas mass as a function of radius. (C) Mass fractions of atomic hydrogen and molecular hydrogen. (D and E) Temperature evolution and the mass-weighted radial velocity of the baryons, respectively. The bottom line with solid symbols in (E) shows the negative value of the local speed of sound at the final time. In all panels the same output times correspond to the same line styles.

pop III stars are massive stars, this gives:

$$\frac{L_*}{L_\odot} = \left(\frac{M_*}{M_\odot}\right)^3 \tag{30}$$

And in combination with equation (28):

$$\frac{t_*}{t_\odot} = \frac{M_*}{M_\odot} / \left(\frac{M_*}{M_\odot}\right)^3 \rightarrow \frac{t_*}{t_\odot} = \left(\frac{M_*}{M_\odot}\right)^{-2} \tag{31}$$

Which is equation (27). So equation (27) is a very good approximation also for pop III stars and the assumption is that the error is negligible.

6.2 Freefall time

We can calculate the freefall time with the formula:

$$T_{ff} = \sqrt{\frac{3\pi}{32G\rho(m)}} \quad s \tag{32}$$

This formula gives us an indication of the speed of the collapse of the cloud. From equation (32) it is easy to see that a denser cloud will collapse faster. Also from equation (32) follows that without counter pressure the collapse is a runaway process, because if a cloud collapses it will become denser and so collapse faster and so on. But this is not a physical situation since there is always counter pressure in the form of gas pressure and radial velocity and radiation pressure can also provide a counter pressure to the gravitational pressure. This is why the freefall time is only an indication for the speed of collapse, in reality collapse times will always be longer.
For the cloud considered in this paper we have, assuming all other species than neutral hydrogen are negligible , $n = 10^3\ cm^{-3}$ which gives $\rho(m) = 1.673 \times 10^{-21}$ g cm^{-3}. And so equation (32) yields $T_{ff} = 1.63 \times 10^6$ yr for the cloud considered here.

6.3 Cooling time

The cooling time is an important factor in cloud collapse. This is basically because when the cloud collapses the potential energy (PE) decreases. But energy conservation requires that the total energy stays the same. Now without cooling this would mean that the kinetic energy (KE) increases by the decrease in potential energy thus the temperature would rise, implying an increase in the gas pressure. We can clearly see this from the mathematical forms. Where the kinetic energy of the cloud is:

$$\langle KE \rangle = \frac{3}{2} kTnV \propto T, \tag{33}$$

with k the boltzman constant, T the gas temperature, n the number density and V the volume of the cloud. The kinetic energy is proportional to T because n scales as $\frac{1}{V}$.
And gas pressure:

$$P = nkT \propto nT \tag{34}$$

From equation (33) it is clear that when the kinetic energy rises the temperature rises also. Now when the cloud collapses the density will rise as well. So, from equation (34),the gas pressure, which counter balances gravitational pressure, rises in two ways. If the only change in the cloud is collapse then the gas pressure will balance the gravitational pressure very soon after the start of collapse, and stop the collapse. It is obvious from equations (33) and (34) that the only way to reduce the gas pressure, to have a continuous collapse, is by lowering the temperature. This can be achieved by radiating away the energy of the particles in the cloud. The cooling time is a measure of how effective a cloud radiates energy. From previous sections we already know that, for low temperatures in a primordial gas, H_2 is the only particle which is able to cool significantly. The cooling time is the time it takes for a cloud to radiate all its energy. So

$$\text{Cooling Time}(T_{cool}) = \frac{\text{Total energy(TE)}}{\text{Total cooling rate}} \tag{35}$$

The total energy is the kinetic energy plus the potential energy. With the potential energy

$$\langle PE \rangle = -\frac{3GM^2}{5R} \tag{36}$$

With G the gravitational constant, M the mass and R the radius. Zeilik et al. (1992).
The total cooling rate is the cooling function (Λ) times the volume. Tiné et al. (1998) have fitted analytical functions to their calculations of the H_2 cooling rates. They did not fit the cooling function itself but the cooling rate coefficient L (ergs cm^3 s^{-1}) which is defined as

$$\Lambda = Ln(H_2)n(H) \tag{37}$$

they found

$$\frac{1}{L} = \frac{1}{L_0} + \frac{n}{\mathcal{L}} + \frac{1}{L_0}\left(\frac{n}{\alpha}\right)^{\beta} \frac{\alpha L_0}{\mathcal{L}}, \tag{38}$$

with

$$\log(L_0^{H_2-H})(T) \begin{cases} -25.87 - \frac{223.0}{T} + 0.179 \log T & \text{if } T \leq 60\text{K}, \\ -31.48 - \frac{117.7}{T} + 2.375 \log T & \text{if } 60\text{K} \leq T \leq 700\text{K}, \\ -28.44 - \frac{1175.7}{T} + 1.830 \log T & \text{if } T \geq 700\text{K}, \end{cases} \tag{39}$$

and

$$\log(\mathcal{L})(T) \begin{cases} -22.06 - \frac{225.2}{T} - 0.551 \log T & \text{if } T \leq 60\text{K}, \\ -30.64 - \frac{121.1}{T} + 3.250 \log T & \text{if } 60\text{K} \leq T \leq 700\text{K}, \\ -22.54 - \frac{1712.6}{T} + 1.234 \log T & \text{if } T \geq 700\text{K}. \end{cases} \tag{40}$$

α and β were then determined by fitting formula (38) for a grid of temperatures to their actual numerical results for the cooling as a function of n. The results are displayed in figure (4). This figure also displays the maximum error of the fit.

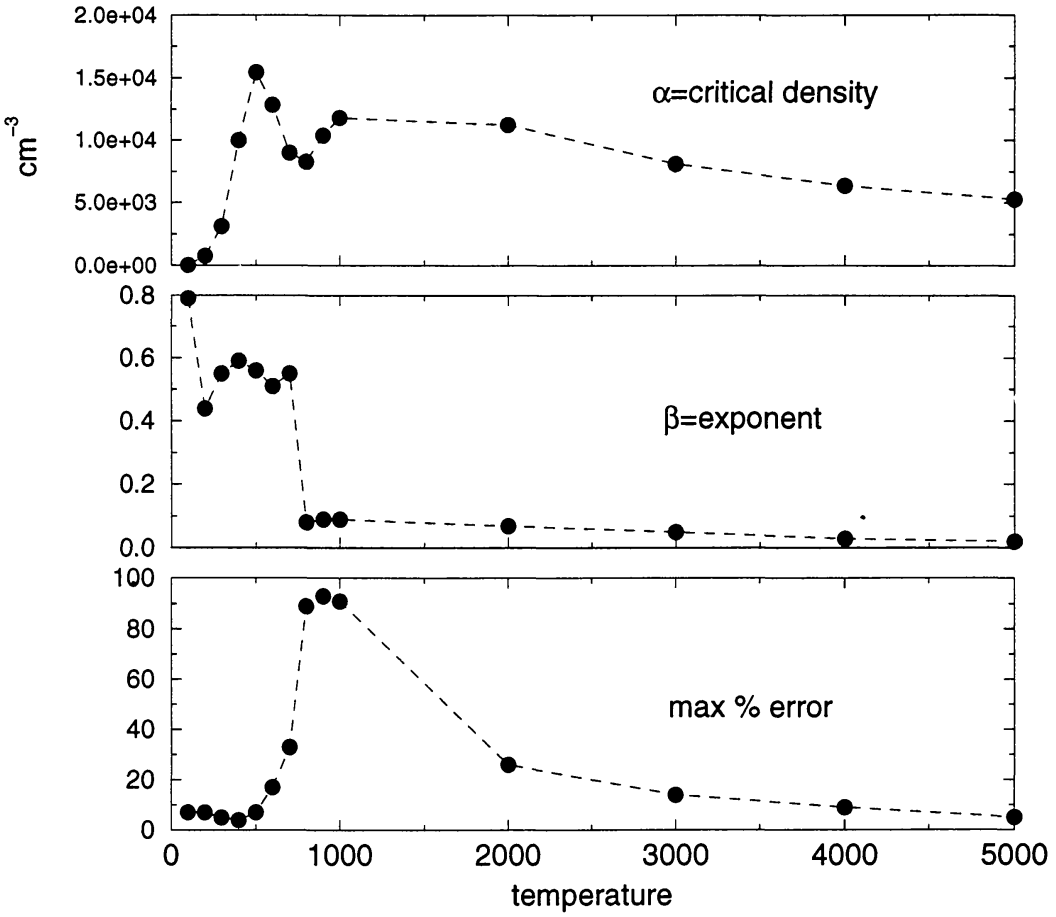

Figure 4: Figure 4 from, Tiné et al. (1998). Top/middle panel fitting coefficient α/β, as a function of temperature, for the cooling rate coefficient L of H_2 immersed in an H bath. Lower panel maximum percentage error of the fit (see text).

The fitting coefficients can be fitted easily to some simple law as function of temperature. To illustrate this figure (5) gives the values from Tiné et al. (1998) (crosses) between 0 and 700 K fitted with an IDL spline (line) for α. For T=0, $\alpha = 0$ is assumed. We fit an IDL spline to β in figure (6), where for T=0, $\beta = 1$ is assumed.

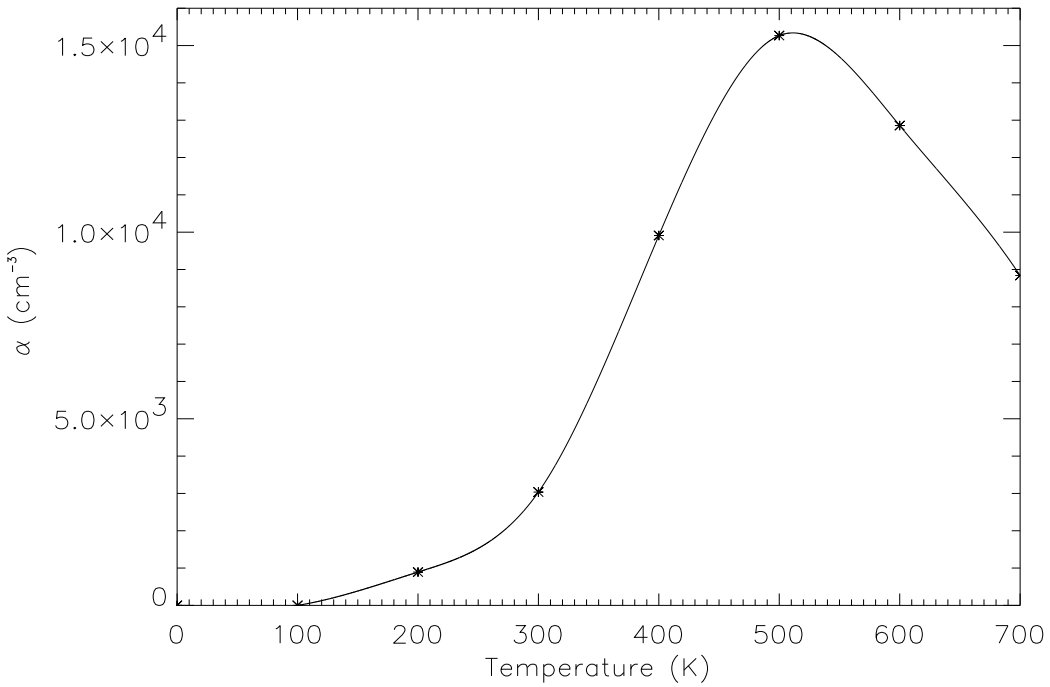

Figure 5: IDL spline (line) fitted over values from Tiné et al. (1998)(crosses) for α between 0 and 700 K

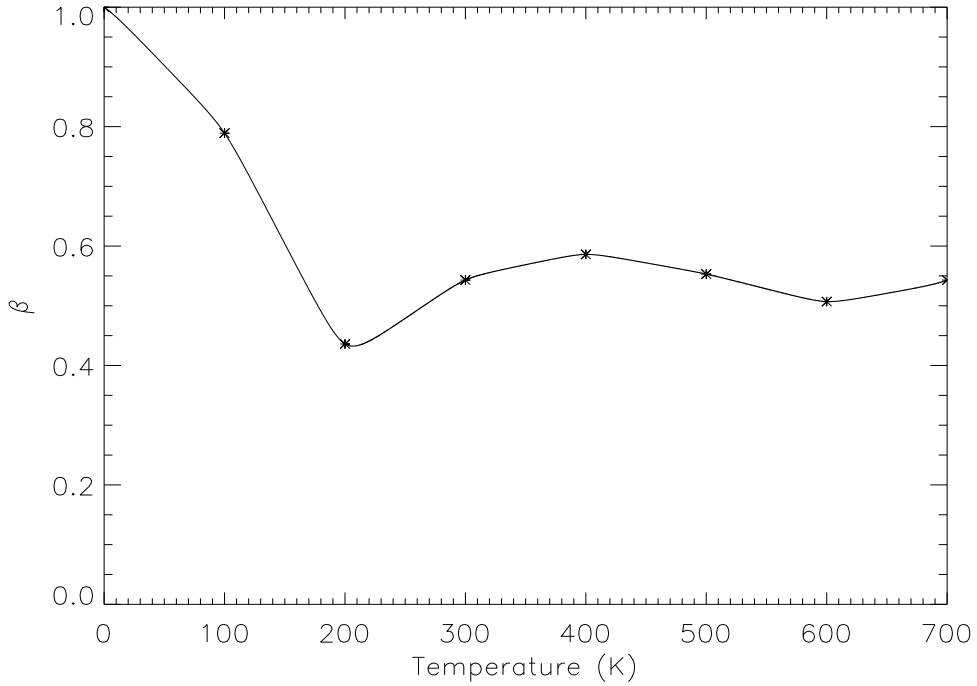

Figure 6: IDL spline (line) fitted over values from Tiné et al. (1998)(crosses) for β between 0 and 700 K

6.4 Timescales for the cloud

Eventually all of this means that the cloud considered here has a freefall time of $T_{ff} = 1.63 \times 10^6\ yr$ and a cooling time of $T_{cool} = 1.97 \times 10^6\ yr$ so we see that the freefall time is

of the order of the cooling time. Because the real collapse time will always be longer than the freefall time (see section 6.2), we can assume that the cloud is unstable under collapse. Lifetimes for the stars considered in the simulations are already given in table (2).

7 Instability criteria

Since the aim is to see if a proto pop III cloud also collapses in the presence of a pop III star radiation field a criterium is needed. There are many different criteria to establish whether the cloud is unstable under collapse. Some of them are, potential energy bigger than the kinetic energy, freefall time longer than cooling time, gravitational pressure larger than the gas pressure and others. Since all of these criteria are approximate and since for the cloud considered here these values are all about the same magnitude a different approach is taken here. In figure (3) the values for a collapsing cloud outside a radiation field are given in seven steps (see Abel et al. (2002)). With these values the potential and kinetic energy of every step can be calculated and so the amount of energy that needs to be irradiated. These equations (37)-(40) yield a minimum H_2 density needed to continue the cloud collapse.

Table (3) displays the values used to calculate this minimum H_2 density. As the energy

Step	T(K)	n(H) (cm^{-3})	n(H_2) (cm^{-3})	Time (years)
1	200	1.0×10^3	1	9×10^6
2	250	1.0×10^6	1×10^3	3×10^5
3	700	1.0×10^8	1×10^5	3×10^4
4	400	1.0×10^9	1×10^6	3×10^3
5	720	1.0×10^{10}	1×10^7	1.5×10^3
6	600	6.0×10^{10}	4×10^{10}	2×10^2
7	700	1	1×10^{13}	no next step
Calculated Values				
Avg. step	Avg. T (K)	Avg. n(H) (cm^{-3})	Energy excess (erg)	Λ (erg s^{-1} cm^{-3})
1-2	225	5.0×10^5	2.7×10^{44}	6.2×10^{-26}
2-3	475	5.0×10^7	3.1×10^{44}	2.1×10^{-21}
3-4	550	5.5×10^8	3.5×10^{45}	2.4×10^{-17}
4-5	560	5.5×10^9	4.5×10^{45}	3.1×10^{-15}
5-6	660	3.5×10^{10}	1.2×10^{46}	1.7×10^{-13}
6-7	650	3.0×10^{10}	8.0×10^{46}	8.3×10^{-11}

Table 3: Values for different steps in the simulation of Abel et al. (2002) and their averages between steps (see text).

is radiated away between two steps the cloud changes over this period, that is why the averages between two steps are taken to calculate the minimum densities. These averages are obtained in the simple way of adding up the values of two steps and divide them by two. This is of course a very rough way of taking the average but due to the large uncertainties in other parts of the problem it is reasonable to assume that a more accurate average will not affect the conclusions. Figure (7) shows the minimum density of molecular hydrogen needed to radiate the increase in energy between steps (black line). As seen from figure (7) this minimum already is very close to the actual averaged density (dashed line) and above the non-averaged density (dotted line). This shows that the simulations without a radiation field are already limited by the amount of molecular hydrogen and its cooling capabilities. This indicates that if molecular hydrogen is dissociated in the cloud the cloud will no longer collapse. Figure (8) shows the same as figure (7) only zoomed into the lower densities. From comparison of the two figures it may seem that differences are larger for the first few steps but notice that the Y-axis is logarithmic in both plots.

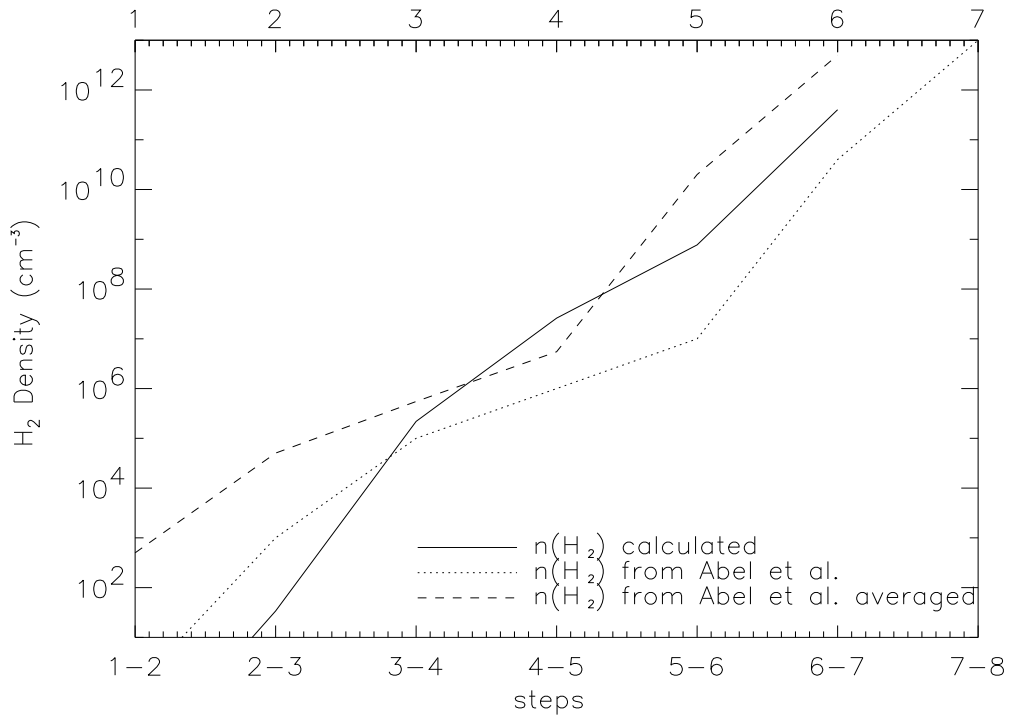

Figure 7: displays minimum amount of molecular hydrogen needed to radiate away the energy increase between two steps(black line, bottom x-axis), average (see text) molecular hydrogen density from Abel et al. (2002)(dashed line, bottom x-axis), molecular hydrogen density from Abel et al. (2002)(dotted line, top x-axis).

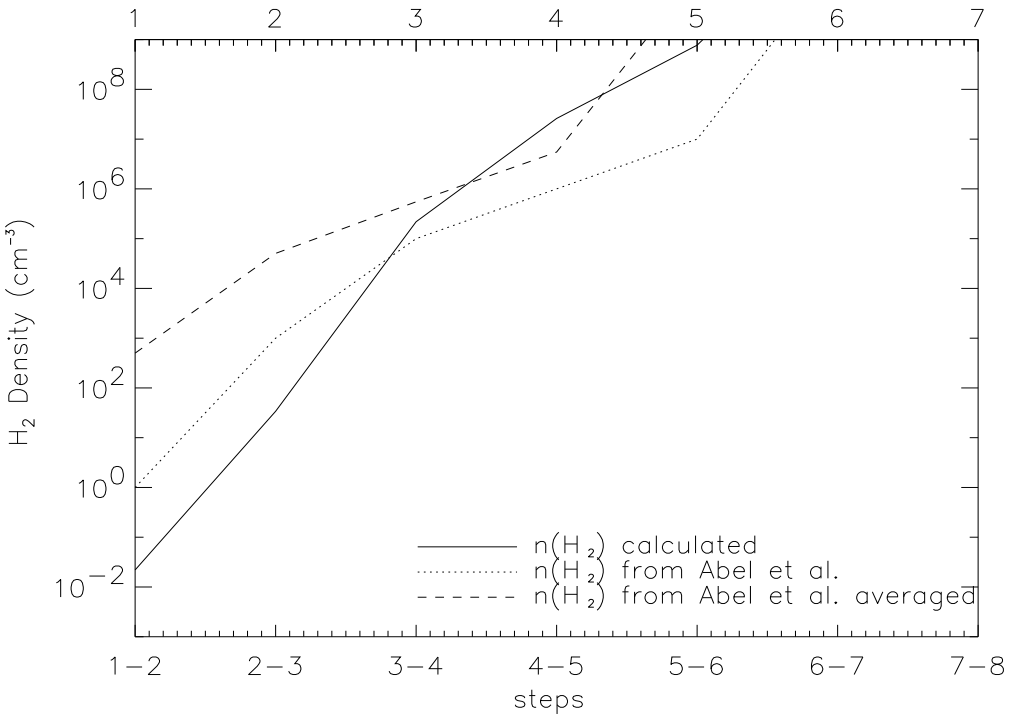

Figure 8: Same as figure (7).

8 Simulations

Several runs were made with an analytic IDL code (see appendix B). Runs were made at distances of 100,50,10,5 and 3 pc where the runs at 100 and 50 pc resemble a different cloud and the runs at 10,5 and 3 pc resemble a situation where fragmentation appeared in an even larger cloud. The inner 0.5 pc of the cloud from Abel et al. (2002) is considered and is assumed to have constant density. The core is divided in 20,000 steps of 7.715×10^{13} cm. In this section the runs on the average between steps in Abel et al. (2002) are presented and discussed. For radiation fields the temperature selected stars are used. The results of steps 1 and 2 and a run with averages with the mass selected sample as radiation fields are presented in the appendix and lead to the same conclusions.

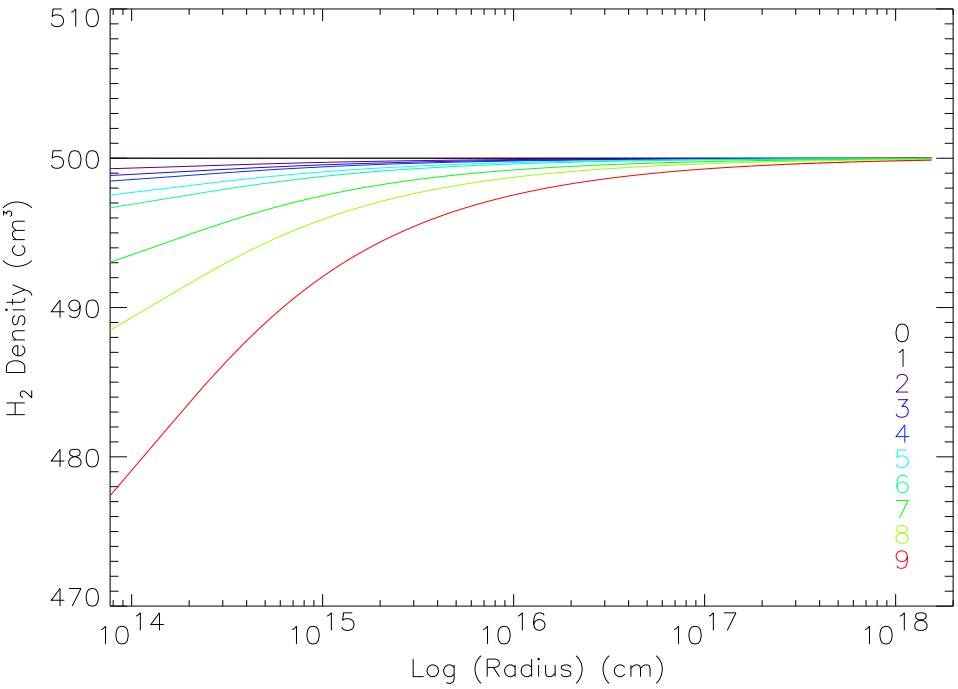

Figure 9: H_2 abundances in the cloud after 9 million years of irradiating the cloud at a distance of 100 pc with numbers 0-9 corresponding to stellar temperatures of 20,000, 30,000, 75,000, 80,000, 85,000, 90,000, 95,000, 100,000, 105,000, 110,000 K. The center of the cloud lies at 1.54×10^{18} cm

From the plots it can be seen that at all distances the amount of H_2 is being reduced. This is as expected since the dissociation is only dependent on the H_2 column density whereas the formation is dependent on the neutral hydrogen column density which is much higher. "Normal" stars (20,000, 30,000 K) have a small influence at any distance. This is also as expected because these black bodies produce relatively little to no far-UV radiation. This leads us to believe that the simulations are correct and the trends are real.
It is easily seen that at a distance from 10-100 pc the influence is so small that there is little effect on the cloud to be expected. But at a distance of 5 pc (figure 13) the hottest star has dissociated a reasonable amount of H_2. And at a distance of 3 pc (figure 13) the three hottest stars (100,000, 105,000, 110,000 K) have dissociated the H_2 from half way (100,000 K) to the center of the cloud (110,000 K). For these cases it is expected that collapse will be halted. Although there main sequence lifetime is calculated to be shorter than 9 million years it is expected that these stars dissociate H_2 fast enough to stop collapse in their lifetimes. To check this we have performed calculations which stopped when the cloud was completely deprived of molecular hydrogen with the cloud at a distance of 5 pc and 10 pc. Table (4) shows the time the different stars from the temperature selected sample needed

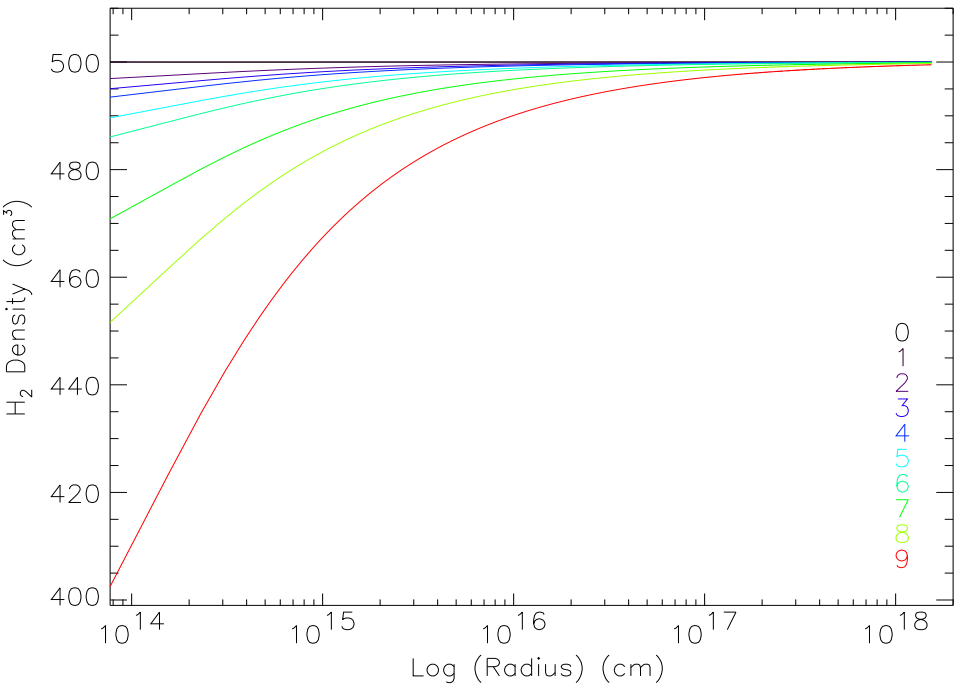

Figure 10: Same as figure (9) except the cloud is at a distance of 50 pc.

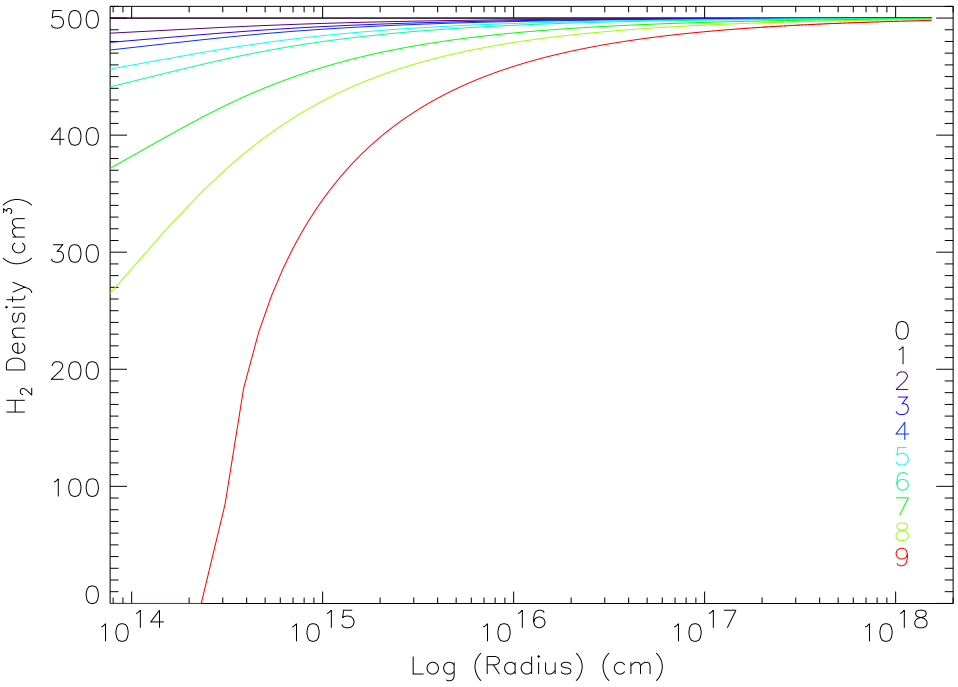

Figure 11: Same as figure (9) except the cloud is at a distance of 25 pc.

to dissociate all the molecular hydrogen in a cloud with n(H)=10^3. As seen in table (4) the time to dissociate all the molecular hydrogen is far shorter than the lifetime of every star. Also the stars above 100,000 K dissociate the H_2 so fast that this lowest density seems to

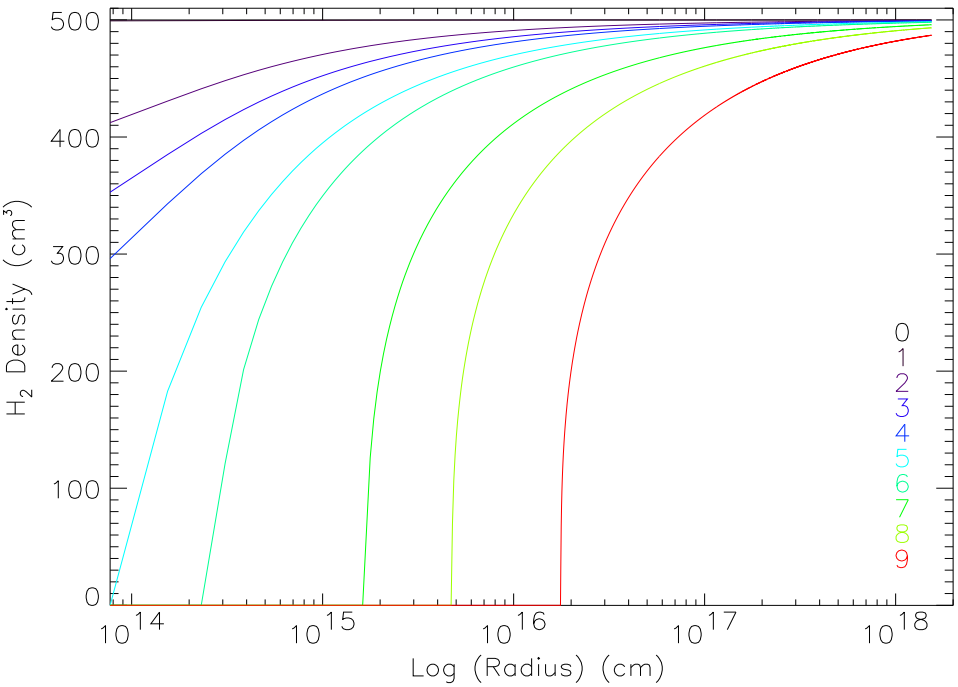

Figure 12: Same as figure(9) except the cloud is at a distance of 10 pc.

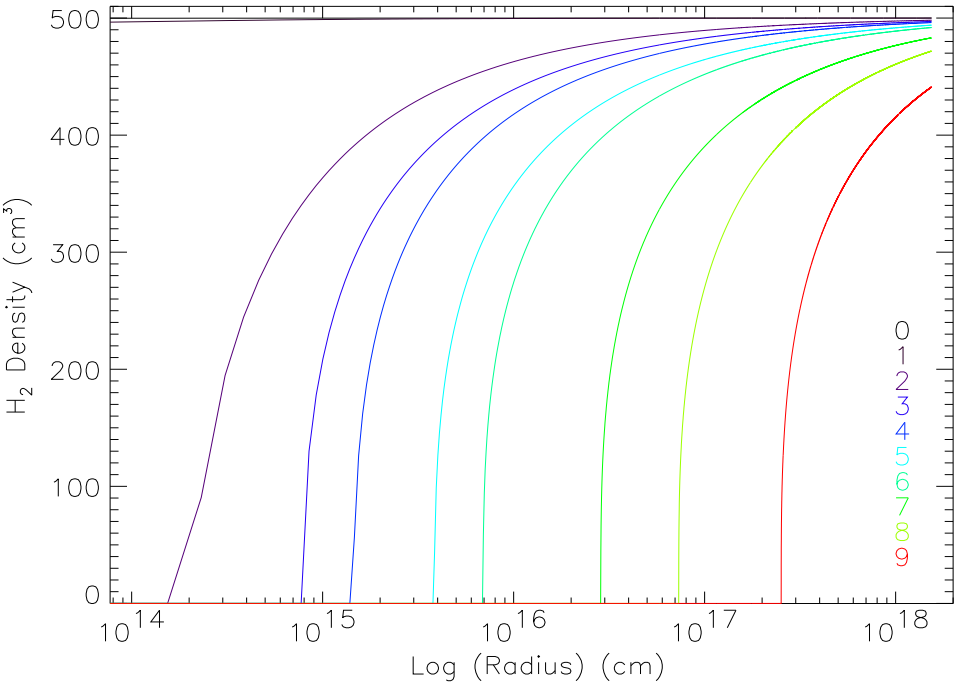

Figure 13: Same as figure (9) except the cloud is at a distance of 5 pc.

be a better approximation than the average for the brightest stars. But of course a cloud in reality will not always be exactly at the beginning of its collapse as a neighborings star turns on. That is why the results from the average are also very interesting. Taking into

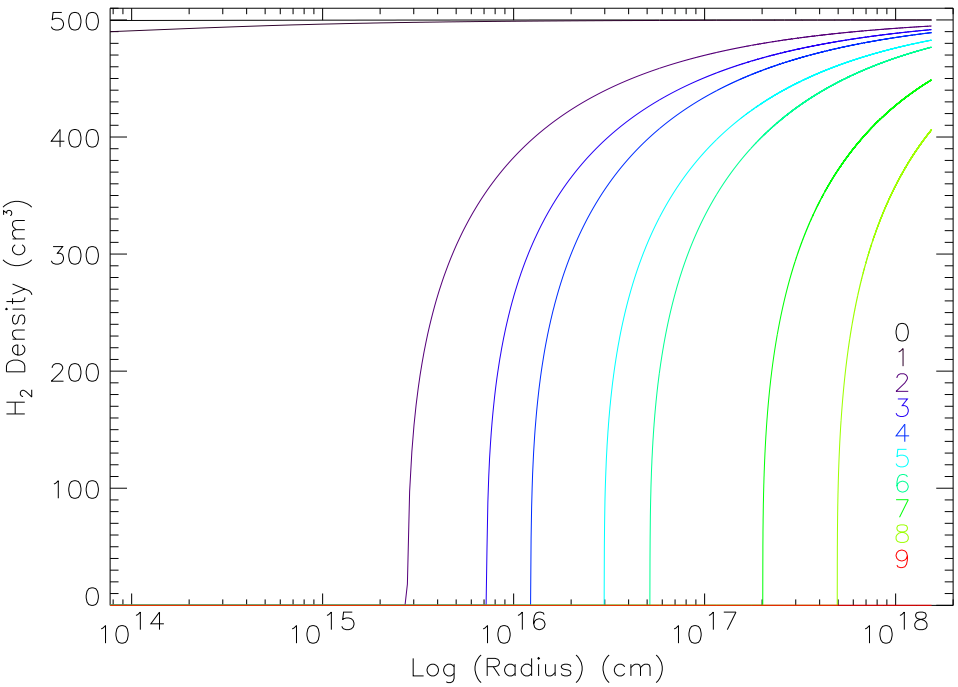

Figure 14: Same as figure (9) except the cloud is at a distance of 3 pc.

Temperature	Lifetime (years)	Time at 10 pc (years)	Time at 5 pc (years)
75×10^3	1.60×10^7	1.80×10^5	4.95×10^4
8×10^4	8.65×10^6	1.17×10^5	3.24×10^4
85×10^3	6.25×10^6	9.13×10^4	2.56×10^4
9×10^4	2.78×10^6	6.03×10^4	1.71×10^4
95×10^3	2.04×10^6	4.63×10^4	1.30×10^4
1×10^5	5.03×10^5	2.38×10^4	7.20×10^3
105×10^3	2.10×10^5	1.57×10^4	4.95×10^3
11×10^4	6.22×10^4	9.00×10^3	2.70×10^3

Table 4: Effective temperatures,Lifetimes of the stars and the time the stars need to dissociate all the H_2 at 10 pc and 5 pc in a cloud with n(H)=10^3.

account that the heavy pop III stars have an asymptote of 110,000 K we can assume that these stars are isolated stars for a range somewhere between 10±2 pc. Looking at these distances pop III double stars will be out of the question as long as they are massive stars, e.g see Omukai & Yoshii (2003). The accuracy of the simulations is estimated to be roughly a factor of two. Due to computational limitations the ionization of neutral hydrogen was calculated with an time-independent column density instead of a time-dependent one, so it was not allowed to eat its way into the cloud. This leads to lower H_2 formation rates in the center of the cloud since the ionizing radiation is not allowed to penetrate the cloud any further at later times, but looking at dissociation and formation rates in the first few time steps this effect is expected to be small if the ionization front penetrates the cloud slightly. If the ionization front penetrates the cloud deeply all H_2 behind the front will be destroyed and thus it will just speed things up. In general these fronts have a low velocity and thus the time-independent approximation is justified. This is why it is believed that taking a time-dependent ionization of atomic hydrogen will not affect the conclusions. The formulas used in these simulations fall outside these areas and the formulas are expected to be quite exact (± 5% error)in the considered parameter regions.+

The fact that we take a bare core of 0.5 pc also introduces an uncertainty since this is not an expected physical situation. A real cloud is not expected to be homogeneous and fragmentation is a problem that must be considered. All in all these uncertainties are not expected to introduce an unacceptable error ($\pm$ 20%).

9 Conclusions

A proto-stellar cloud was taken from Abel et al. (2002) and put in a radiation field which is meant to resemble a pop III star. Twenty different radiation fields were considered. Due to computational limitations it was only possible to consider the inner 0.5 pc of the cloud. The cloud is divided in 20,000 steps of $7.715 \times 10^{13} cm$. The abundance of H_2 is followed throughout the cloud for 9 million years. It is found that for the radiation fields which theorists expect for the general pop III stars these stars will be isolated in areas with a 10 ± 2 pc radius as long as there is no fragmentation within the proto stellar core and they radiate at effective temperatures above 100,000 K. We have established a criterium for cloud collapse which is that if a reasonable amount of H_2 is destroyed the cloud will stop to collapse. There are a few problems with this criterium. The edge between no H_2 at all and the initial amount of H_2 is sharp, this could imply several things. If there is no H_2 left we assume that the cloud is not capable of collapsing. Now what happens if a large part of the cloud is deprived of H_2. Is the part where no H_2 is dissociated still capable of collapse? To answer this question further simulations are required, but we assume that the cloud will not collapse fully if the H_2 is eaten away for more than half of the radius of the cloud. Now the fact that all the molecular hydrogen is dissociated could lead to dynamically passive clouds just hanging around and this can bring down fragmentation masses so the next generation of stars is not so massive, Omukai & Yoshii (2003). These simulations were quite basic because of computational and time limitations and there is still a lot of work to be done. Future simulations should contain time-dependent neutral hydrogen ionization, bigger clouds, fragmentation, 3d simulations and a radiation field produced by several stars surrounding the proto-stellar gas cloud according to a realistic distribution of stars. We do feel that the trends observed in the simulations are real and indicate a negative feedback by the first stars on the second generation so the epoch of reionization will be stretched because star formation will be quenched after the first stars start to radiate. Based on these simulations and literature the epoch of reionization is expected to be a double epoch. The very first stars are massive, deprived of metals and capable of reionizing significant parts of the universe subsequently a next generation of smaller low metallicity stars reionize the universe completely. This is also what the observations performed up to now seem to imply. If the second generation is made up of smaller stars this could also solve the problem of contaminating the IGM in time (Black hole formation, $\gamma - \gamma$ supernovae). There still remain many problems with the whole picture and much more research will be required before the epoch of reionization is understood reasonably well.

References

Abel, T., Anninos, P., Zhang, Y., & Norman, M. L. 1997, New Astronomy, 2, 181

Abel, T., Bryan, G. L., & Norman, M. L. 2002, Science, 295, 93

Abgrall, H., Le Bourlot, J., Pineau Des Forets, G., Roueff, E., Flower, D. R., & Heck, L. 1992, A&A, 253, 525

Abgrall, H., Roueff, E., Launay, F., Roncin, J. Y., & Subtil, J. L. 1993a, A& A suppl., 101, 273

—. 1993b, A& A suppl., 101, 323

Baraffe, I., Heger, A., & Woosley, S. E. 2001, ApJ, 550, 890

Barkana, R. 2002, New Astronomy, 7, 85

Becker, R. H., Fan, X., White, R. L., Strauss, M. A., Narayanan, V. K., Lupton, R. H., Gunn, J. E., Annis, J., Bahcall, N. A., Brinkmann, J., Connolly, A. J., Csabai, I., Czarapata, P. C., Doi, M., Heckman, T. M., Hennessy, G. S., Ivezić, Ž., Knapp, G. R., Lamb, D. Q., McKay, T. A., Munn, J. A., Nash, T., Nichol, R., Pier, J. R., Richards, G. T., Schneider, D. P., Stoughton, C., Szalay, A. S., Thakar, A. R., & York, D. G. 2001, AJ, 122, 2850

Bell, K. L. & Williams, D. A. 1983, MNRAS, 202, 407

Bertoldi, F., Carilli, C. L., Cox, P., Fan, X., Strauss, M., Beelen, A., Omont, A., & R., Z. 2003, astro-ph/0305116v1

Bertoldi, F. & Draine, B. T. 1996, ApJ, 458, 222

Black, J. H. & Dalgarno, A. 1976, ApJ, 203, 132

—. 1977, ApJ suppl., 34, 405

Black, J. H. & van Dishoeck, E. F. 1987, ApJ, 322, 412

Bromm, V., Coppi, P. S., & Larson, R. B. 2002, ApJ, 564, 23

Bromm, V., Kudritzki, R. P., & Loeb, A. 2001, ApJ, 552, 464

Browning, M. K., Tumlinson, J., & Shull, J. M. 2003, ApJ, 582, 810

Cayrel, R. 1996, A& A rev., 7, 217

Cazaux, S. & Spaans, M. 2003, in progress, 1

Chabrier, G. & Baraffe, I. 1997, A&A, 327, 1039

Dalgarno, A. & Stephens, T. L. 1970, ApJ Lett., 160, L107+

de Jong, T., Boland, W., & Dalgarno, A. 1980, A&A, 91, 68

Demircan, O. & Kahraman, G. 1991, Ap& SS, 181, 313

Draine, B. T. 1978, ApJ suppl., 36, 595

Draine, B. T. & Bertoldi, F. 1996, ApJ, 468, 269

Field, G. B., Somerville, W. B., & Dressler, K. 1966, ARA&A, 4, 207

Guenther, D. B. & Demarque, P. 1983, A&A, 118, 262

Haiman, Z., Abel, T., & Rees, M. J. 2000, ApJ, 534, 11

Haiman, Z., Rees, M. J., & Loeb, A. 1996, ApJ, 467, 522

—. 1997, ApJ, 484, 985

Heger, A., Woosley, S., Baraffe, I., & Abel, T. 2002, in Lighthouses of the Universe: The Most Luminous Celestial Objects and Their Use for Cosmology Proceedings of the MPA/ESO/, p. 369, 369–+

Heger, A. & Woosley, S. E. 2002, ApJ, 567, 532

Henry, R. C. 2002, ApJ, 570, 697

Hjellming, R. M. 1966, ApJ, 143, 420

Hollenbach, D. & McKee, C. F. 1979, ApJ suppl., 41, 555

Hui, L. & Haiman, Z. 2003, astro-ph/0302439v3

Hutchings, R. M., Santoro, F., Thomas, P. A., & Couchman, H. M. P. 2002, MNRAS, 330, 927

Jonin, C., Liu, X., Ajello, J. M., James, G. K., & Abgrall, H. 2000, ApJ suppl., 129, 247

Kitayama, T. & Ikeuchi, S. 2000, ApJ, 529, 615

Lee, H.-H., Herbst, E., Pineau des Forets, G., Roueff, E., & Le Bourlot, J. 1996, A&A, 311, 690

Marigo, P., Girardi, L., Chiosi, C., & Wood, P. R. 2001, A&A, 371, 152

Nakamura, F. & Umemura, M. 1999, ApJ, 515, 239

—. 2002, ApJ, 569, 549

Norman, C. A. & Spaans, M. 1997, ApJ, 480, 145

Norman, M. L., Abel, T., & Bryan, G. 2000, in The First Stars. Proceedings of the MPA/ESO Workshop held at Garching, Germany, 4-6 August 1999. Achim Weiss, Tom G. Abel, Vanessa Hill (eds.). Springer., 250–+

Oh, S. P. & Haiman, Z. 2002, ApJ, 569, 558

Omukai, K. & Nishi, R. 1999, ApJ, 518, 64

Omukai, K., Nishi, R., Uehara, H., & Susa, H. 1999, in IAU Symp. 183: Cosmological Parameters and the Evolution of the Universe, 161–+

Omukai, K. & Palla, F. 2001, ApJ lett., 561, L55

Omukai, K. & Yoshii, Y. 2003, astro-ph/0308514v1

Palla, F., Salpeter, E. E., & Stahler, S. W. 1983, ApJ, 271, 632

Ripamonti, E., Haardt, F., Ferrara, A., & Colpi, M. 2002, MNRAS, 334, 401

Saumon, D., Bergeron, P., Lunine, J. I., Hubbard, W. B., & Burrows, A. 1994, ApJ, 424, 333

Saumon, D., Chabrier, G., & van Horn, H. M. 1995, ApJ suppl., 99, 713

Scannapieco, E., Ferrara, A., & Madau, P. 2002, ApJ, 574, 590

Schaerer, D. 2002, A&A, 382, 28

Shull, J. M. 1978, ApJ, 219, 877

Siess, L., Livio, M., & Lattanzio, J. 2002, ApJ, 570, 329

Spitzer, L. J. 1947, AJ, 52, 130

Stecher, T. P. & Williams, D. A. 1967, ApJ Lett., 149, L29+

Suto, Y. & Silk, J. 1988, ApJ, 326, 527

Tiné, S., Lepp, S., & Dalgarno, A. 1998, Memorie della Societa Astronomica Italiana, 69, 345

Tumlinson, J. & Shull, J. M. 2000, ApJ Lett., 528, L65

van Dishoeck, E. F. & Black, J. H. 1986, ApJ suppl., 62, 109

Wolniewicz, L., Simbotin, I., & Dalgarno, A. 1998, ApJ suppl., 115, 293

Yahil, A. 1983, ApJ, 265, 1047

Yan, M., Sadeghpour, H. R., & Dalgarno, A. 1998, ApJ, 496, 1044

Zeilik, M., Gregory, S. A., & Smith, E. V. P. 1992, Introductory astronomy and astrophysics (Fort Worth : Saunders College Pub., c1992. 3rd ed.)

Zvereva, A. M., Severnyi, A. B., Granitskii, L. V., Hua, C. T., Cruvellier, P., & Courtes, G. 1982, A&A, 116, 312

Appendix A: Results

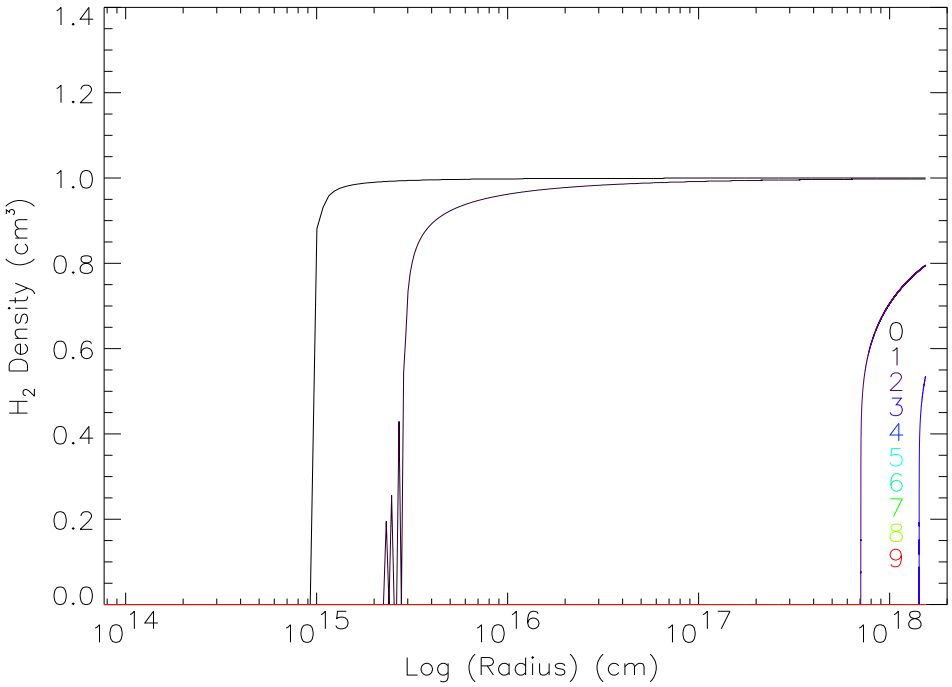

Figure 15: Same as figure (9) except initial n(H_2)= 1 cm^3. Lines not seen are 0 throughout the cloud.

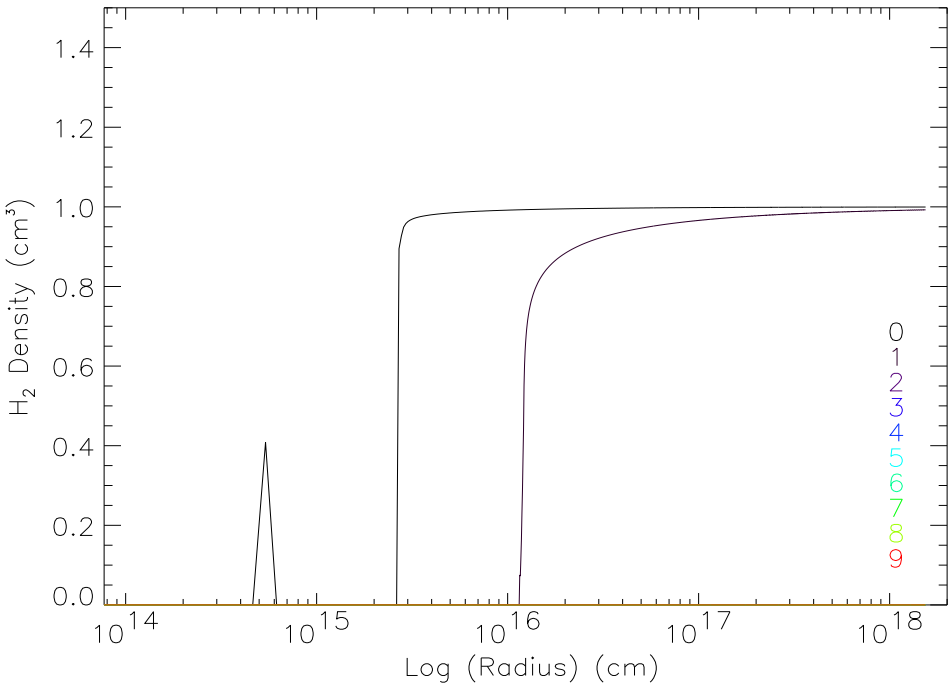

Figure 16: Same as figure (15) except the cloud is at a distance of 50 pc.

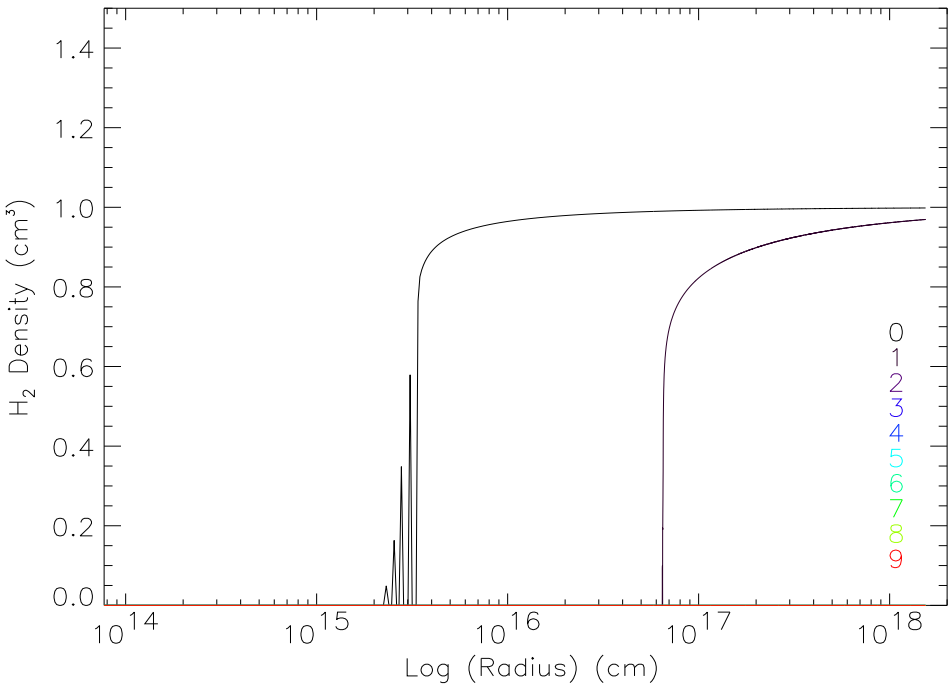

Figure 17: Same as figure (15) except the cloud is at a distance of 25 pc.

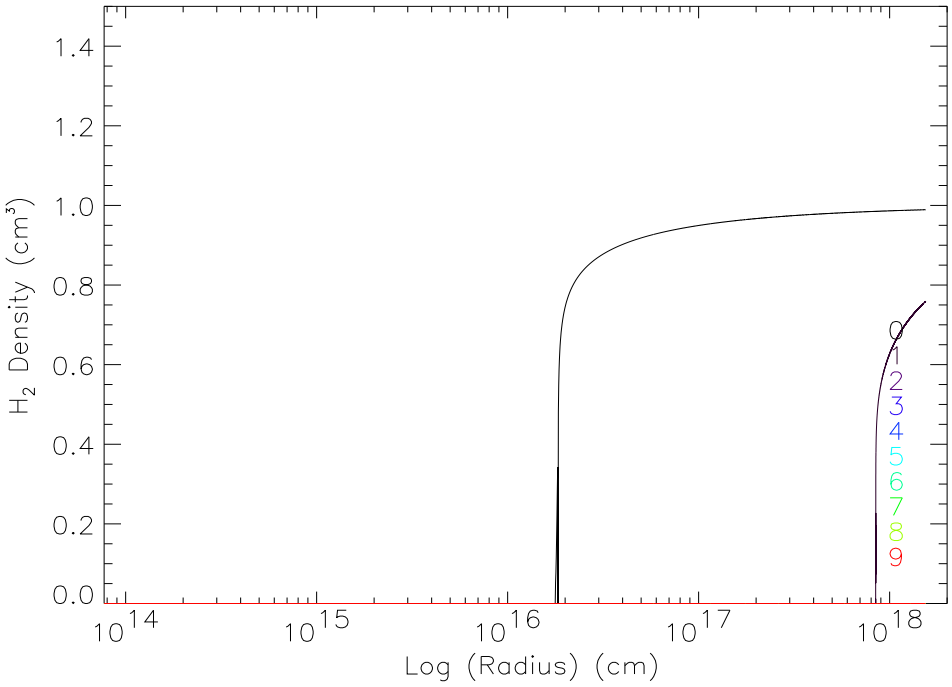

Figure 18: Same as figure (15) except the cloud is at a distance of 10 pc.

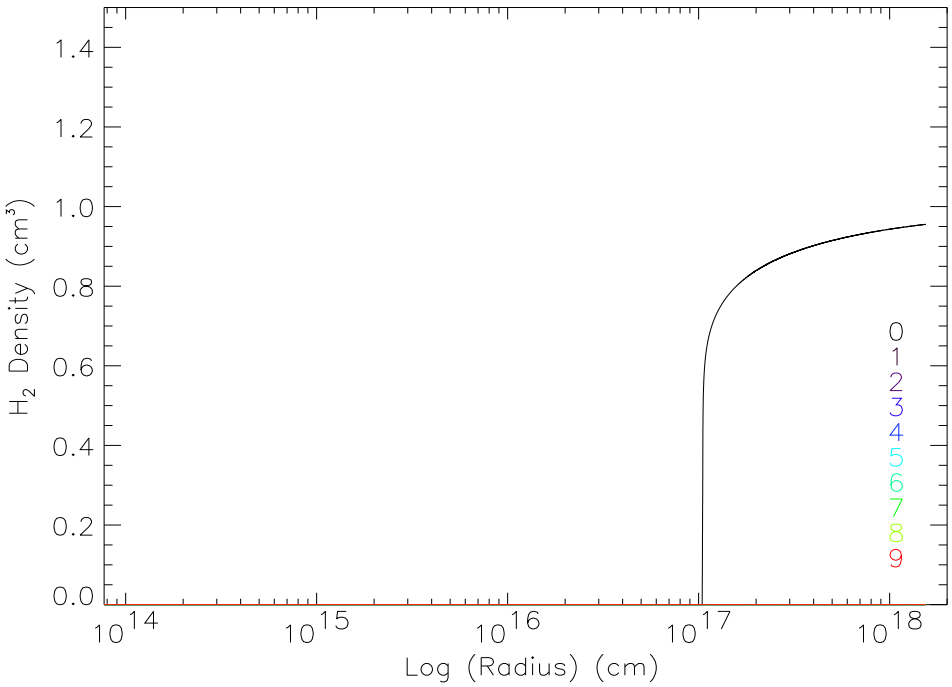

Figure 19: Same as figure (15) except the cloud is at a distance of 5 pc.

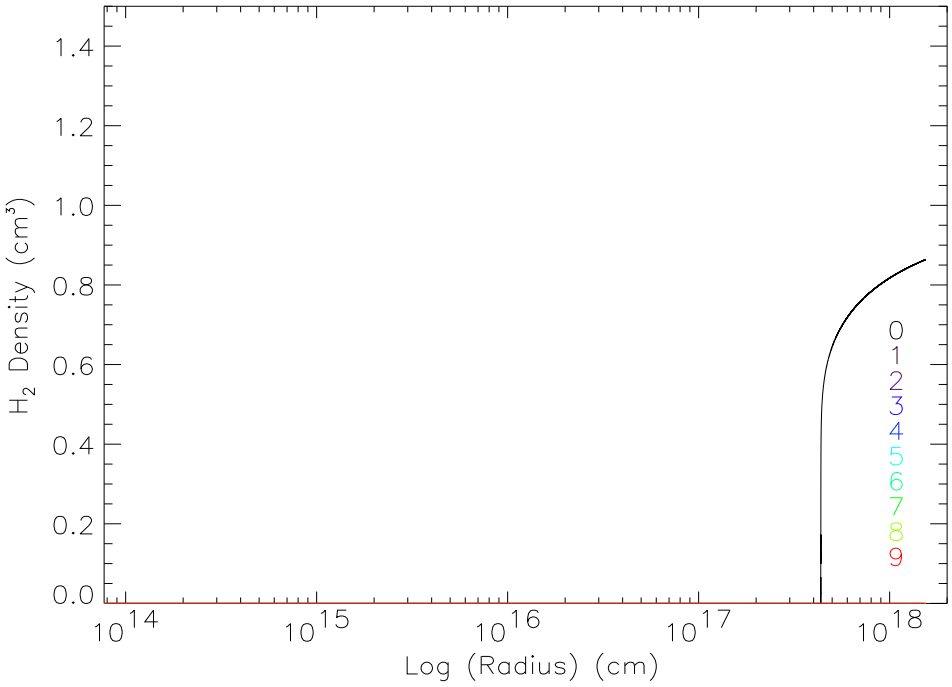

Figure 20: Same as figure (15) except the cloud is at a distance of 3 pc.

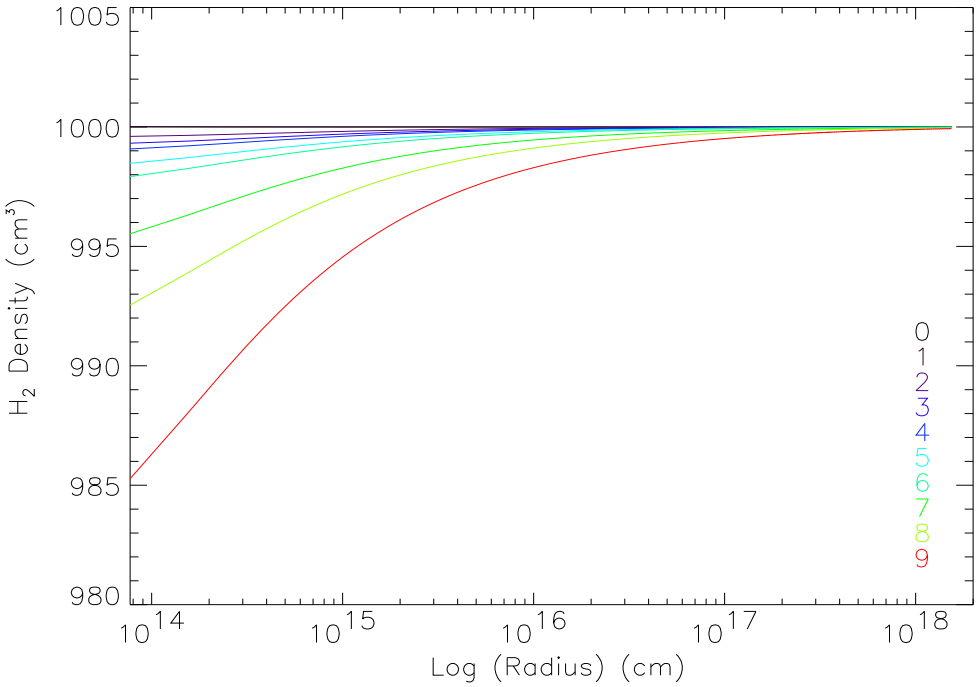

Figure 21: Same as figure (9) except initial n(H_2)= 1000 cm^3.

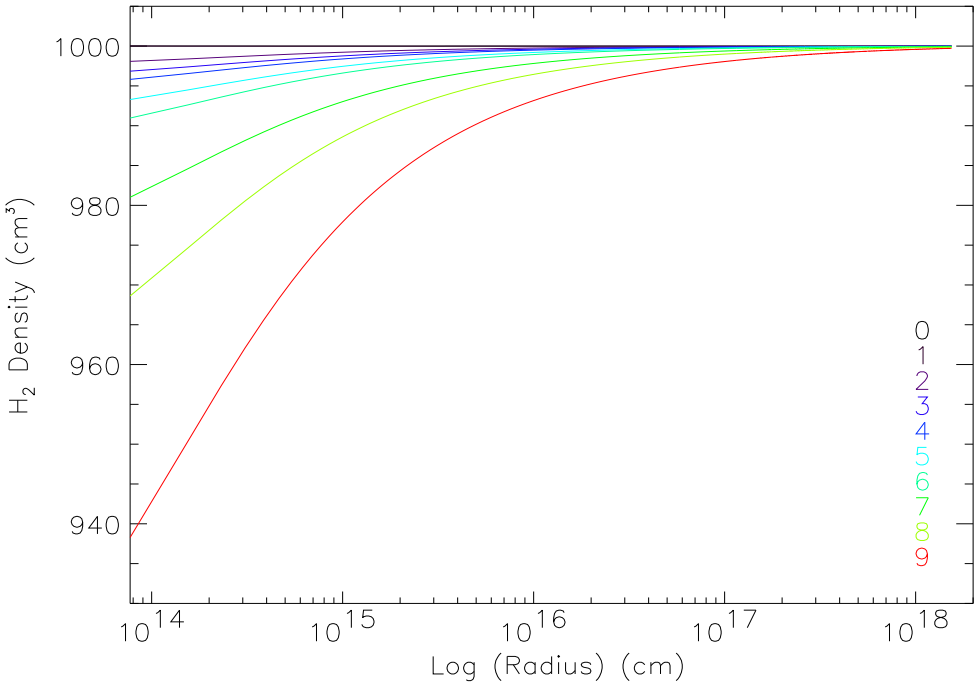

Figure 22: Same as figure (21) except the cloud is at a distance of 50 pc.

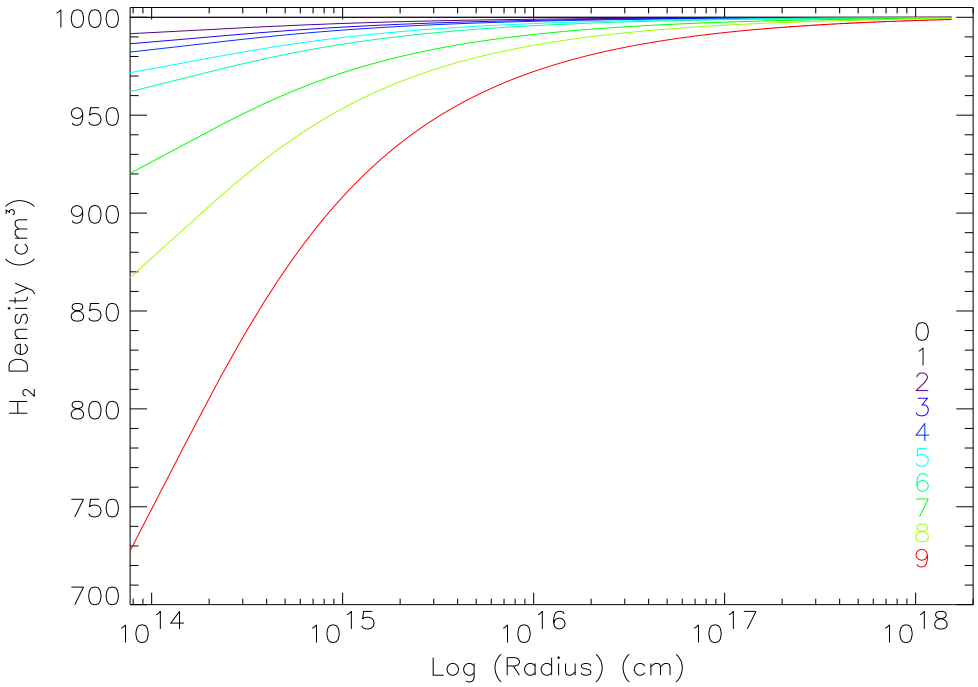

Figure 23: Same as figure (21) except the cloud is at a distance of 25 pc.

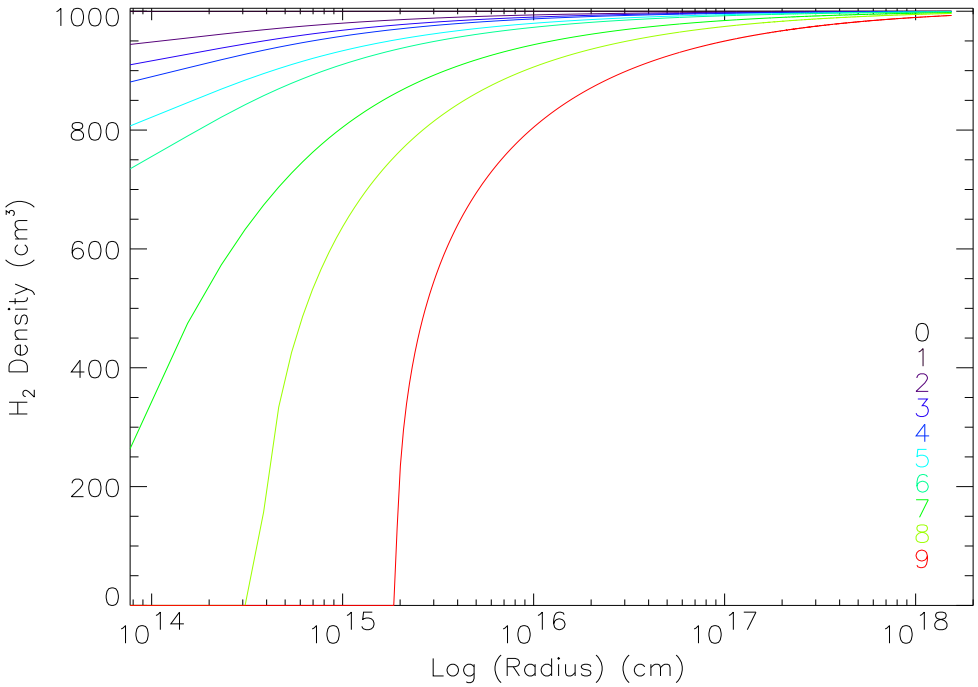

Figure 24: Same as figure (21) except the cloud is at a distance of 10 pc.

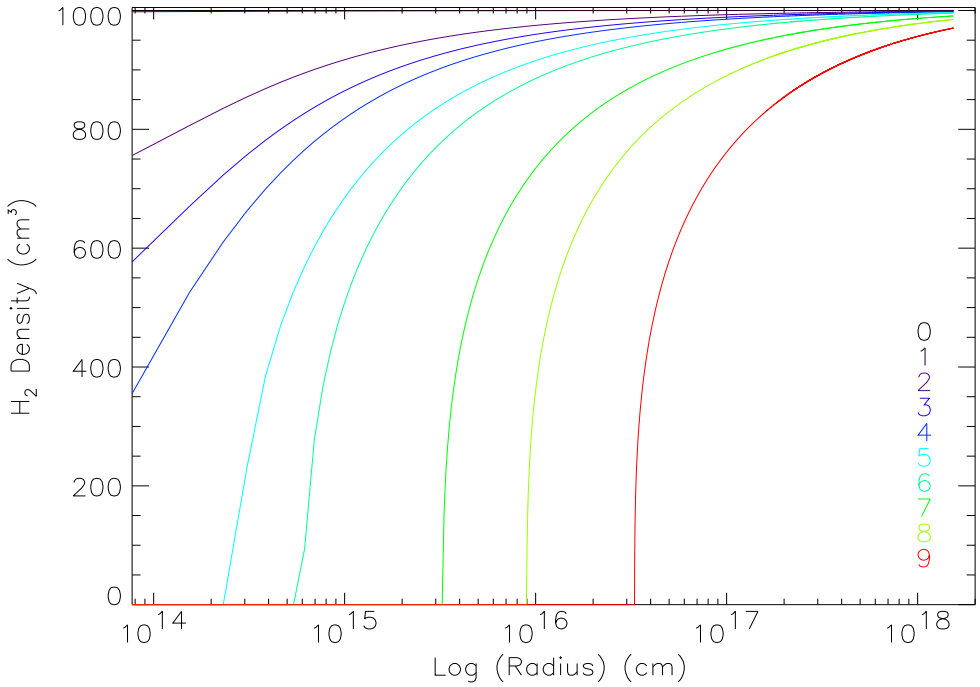

Figure 25: Same as figure (21) except the cloud is at a distance of 5 pc.

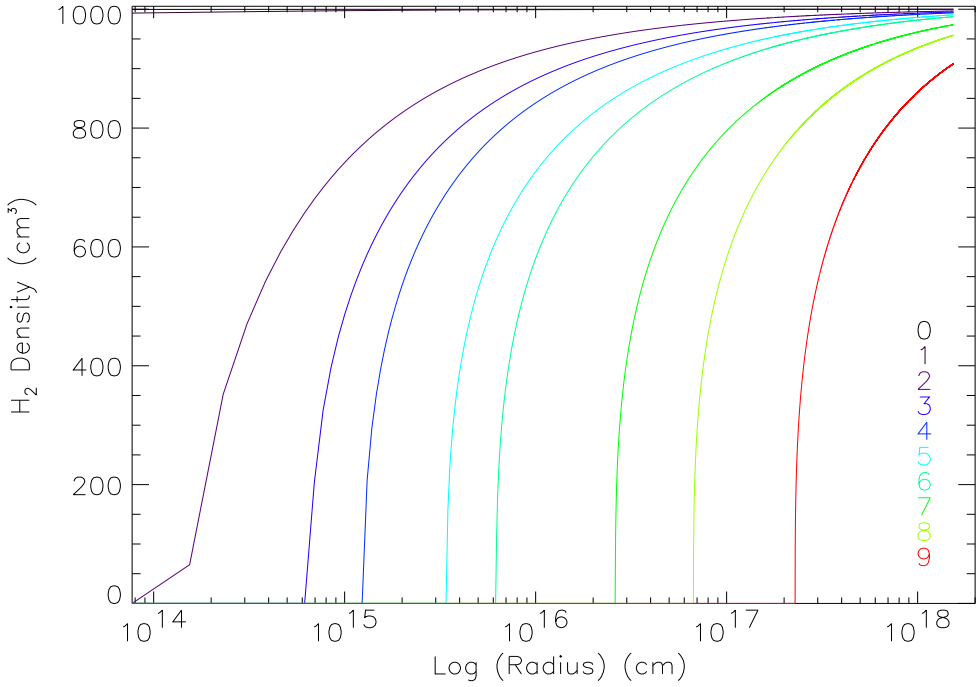

Figure 26: Same as figure (21) except the cloud is at a distance of 3 pc.

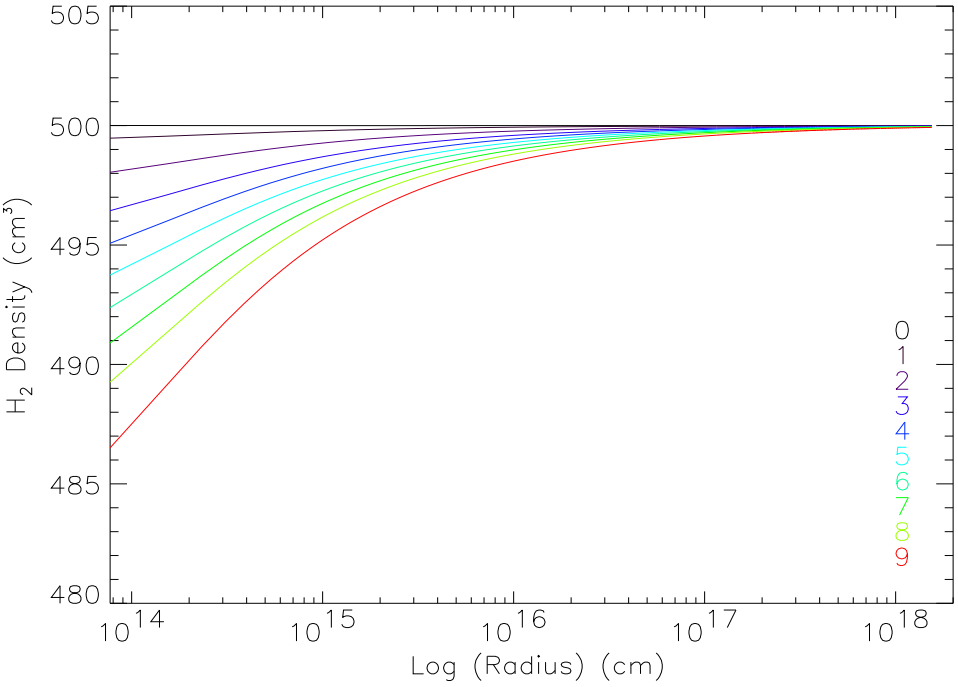

Figure 27: Same as figure (9) except numbers 0-9 are now corresponding to temperatures of 30,000, 72,443, 86,099, 95,499, 97,948, 99,390, 100,818, 102,435, 104,712, 105,715 K.

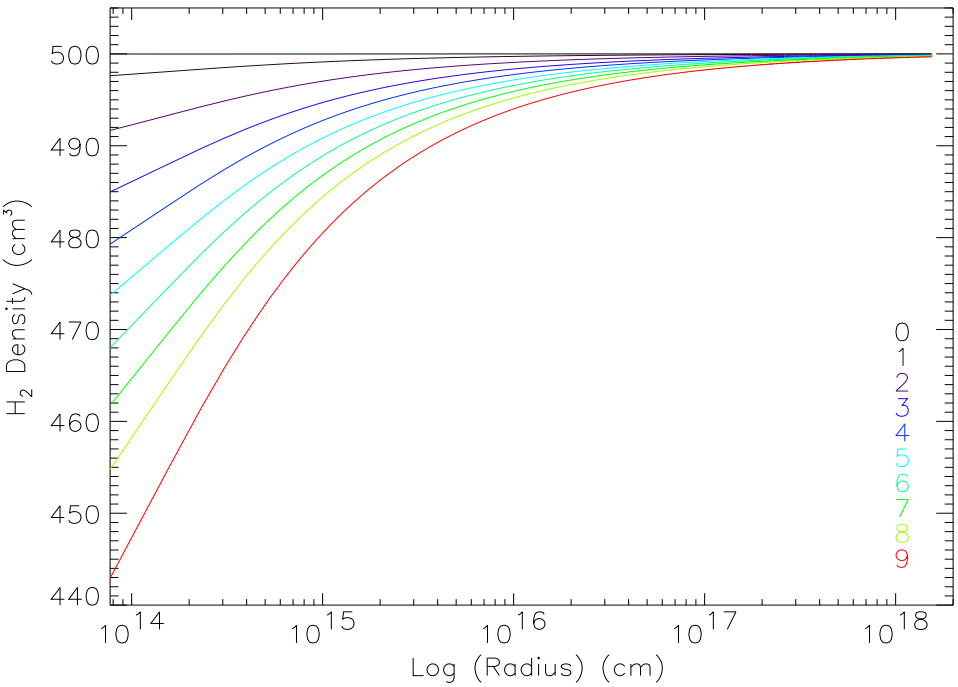

Figure 28: Same as figure (27) except the cloud is at a distance of 50 pc.

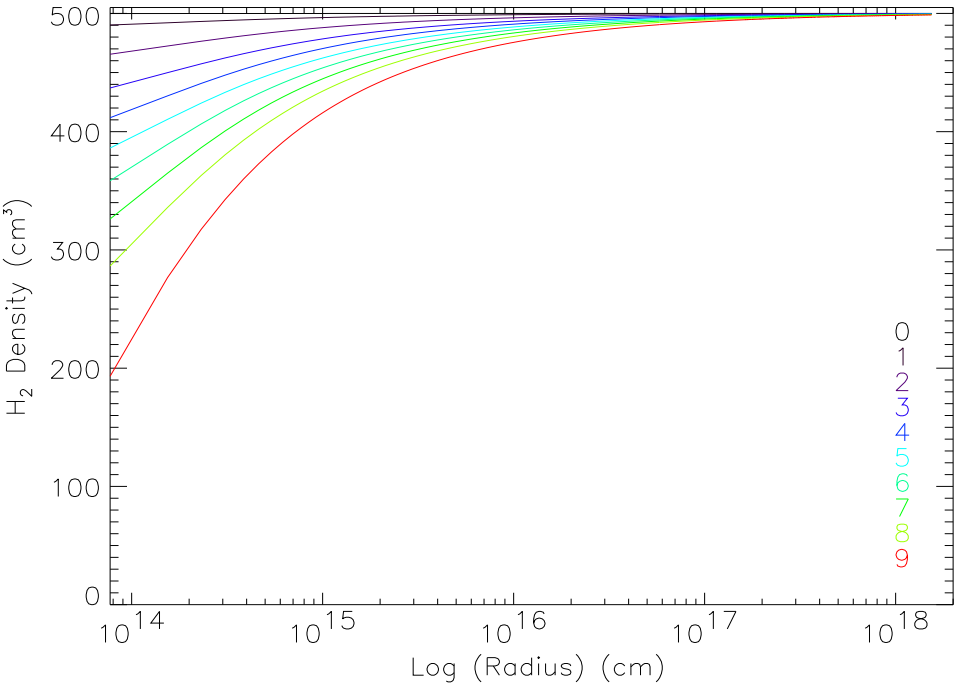

Figure 29: Same as figure (27) except the cloud is at a distance of 25 pc.

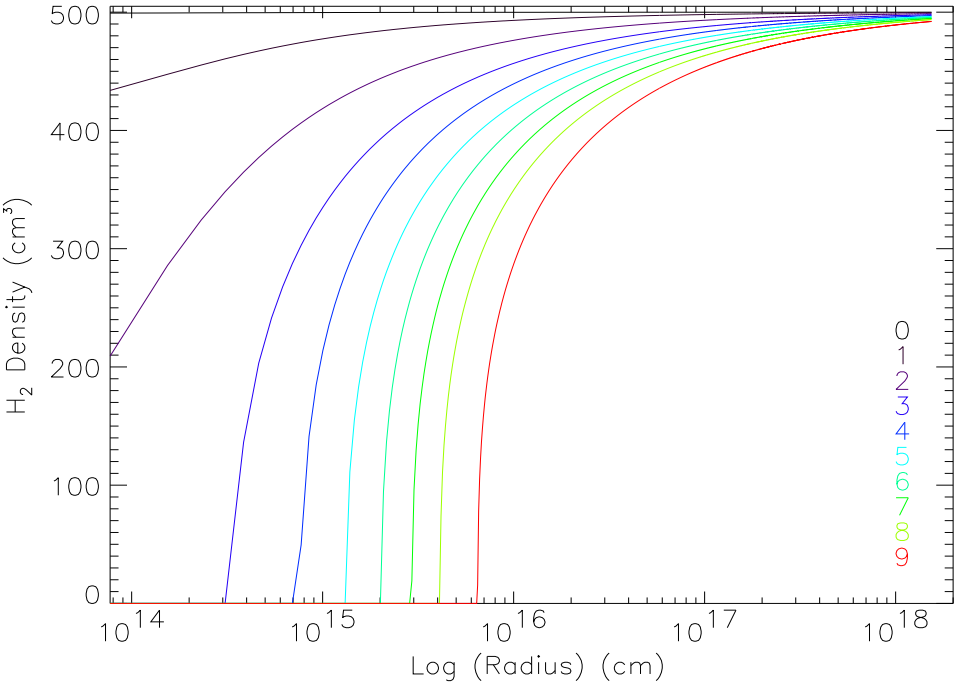

Figure 30: Same as figure (27) except the cloud is at a distance of 10 pc.

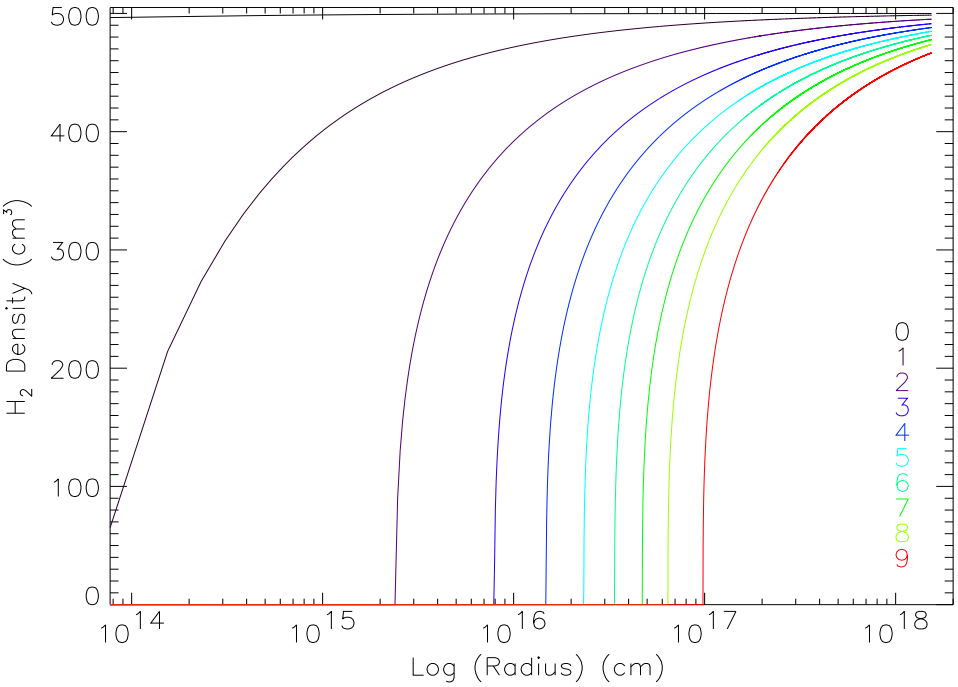

Figure 31: Same as figure (27) except the cloud is at a distance of 5 pc.

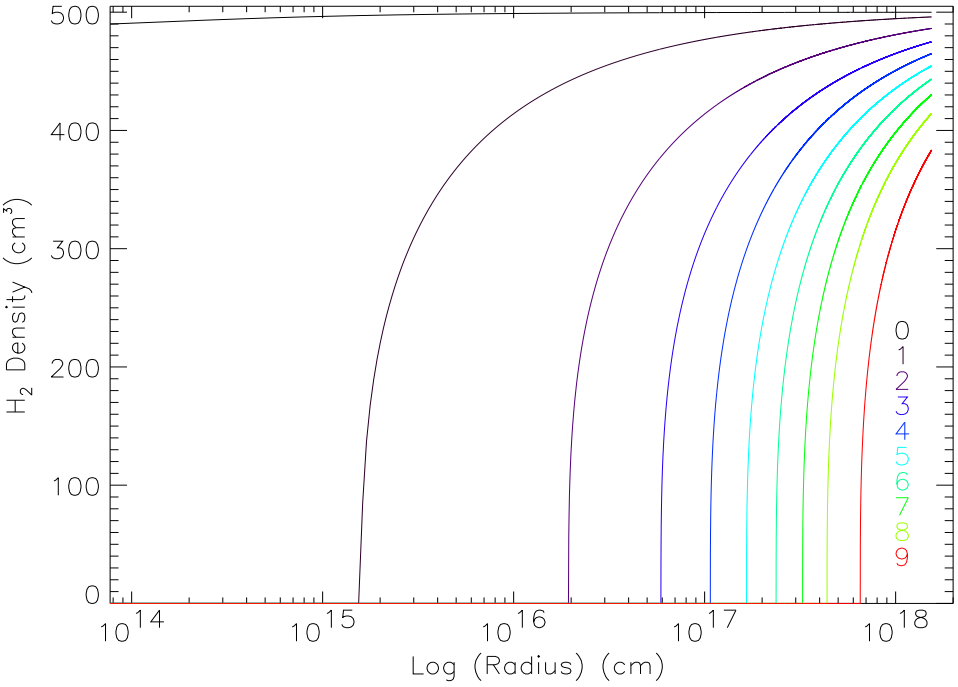

Figure 32: Same as figure (27) except the cloud is at a distance of 3 pc.

Appendix B: The programs

Calculating the solid angle

```
function omega, con


Ra = radius(con)
Ram =dblarr(10)
Ram = Ra * 696000000.
pi = 3.14159265358979

da = pi * Ram^2

r =dblarr(1)
print, 'geef afstand tot de wolk in parsec'
read, r
dOmega = dblarr(10)
rm = r * 3.086E16
for i=0,9 do begin
      dOmega(i) = da(i)/(rm^2)
endfor

return, dOmega
end
```

Calculating the blackbody

```
function blackbody,con

;temperatures

T=temperature (con)
; number of steps must be equal to n in wavelength
n = 20000


In = dblarr(n+1,10)
lam2 = dblarr (n+1)
nu = dblarr (n+1)
;reading in the wavelengths
lam = wavelength(con)


; constants
c = 3E10
h = 6.6260755E-27
k = 1.380658E-16
nu = c/lam


nu2 = dblarr (n+1)


for i=0,n do begin
   nu2(i)= nu(i)^3
endfor
```

```
;calculating the intensity of black bodies at the given temperatures and frequencies
for j=0,9 do begin
      FOR i=0,n DO BEGIN
          In(i,j)= ((2.*h*nu2(i))/(c^2))*(1./(exp((h*nu(i))/(k*T(j)))-1))
      ENDFOR
endfor

return, In

end
```

Calculating wavelengths

```
function wavelength,con

;default step size
;stapgrootte
dx= 0.01E-8


;stapaantal gelijk zijn aan n in blackbody
n = 20000
lam = dblarr(n+1)
;wavelength production
lam(0) = 900E-8
for i= 1,n do begin
   lam(i) = lam(i-1) + dx
endfor
return, lam
end
```

Calculating the H_2 density

```
pro TheBigCahoonawork3

n=20000

; defining arrays
Hdensit= dblarr(n+1,10)
Temp=dblarr(10)
Intensitynu=dblarr(n+1,10)
NHtwo= dblarr(n+1,10)
NHtwo3= dblarr(n+1,10)
NHcolumn = dblarr(n+1,10)
Hdensstep =dblarr(n+1,10)
H = dblarr(n+1)
tau = dblarr(n+1,10)
domega=dblarr(10)
Insert=dblarr(10)
Jto=dblarr(n+1,10)
Rf= dblarr(n+1,10)
nu=dblarr(n+1)
Rd=dblarr(n+1,10)
NHtwostep=dblarr(n+1,10)
NHtwocolumn = dblarr(n+1,10)
Rhalf=dblarr(10)
taudis = dblarr(n+1,10)
x=dblarr(n+1,10)
```

```
efc = dblarr(n+1,10)
Beta=dblarr(n+1,10)
Betaeen=dblarr(n+1,10)
Betatwee=dblarr(n+1,10)
R=dblarr(n+1,10)
Rdhtwo=dblarr(n+1,10)
Rfhtwo=dblarr(n+1,10)
NHtwonew=dblarr(n+1,10)
Hdensitnew=dblarr(n+1,10)
NHTOWO=dblarr(n+1,10)
Rdols=dblarr(n+1,10)
distance= dblarr(n+1)
Intweeeen=dblarr(10)

;reading in distributions
H(*) = 5e5
Temp=temperature(con)
Intensitynu = blackbody(con)
domega=omega(con)
lam = wavelength(con)
dVd= velocity(con)


; constants
d=[0,1,2,3,4,5,6,7,8,9]
b=string(d,format='(i1)')
name = '~/Grootonderzoek/output/NHtwoend410pc'+b+'.dat'
Intensity = [Intensitynu(10000,0),Intensitynu(10000,1),Intensitynu(10000,2)
  ,Intensitynu(10000,3),Intensitynu(10000,4),Intensitynu(10000,5)
  ,Intensitynu(10000,6),Intensitynu(10000,7),Intensitynu(10000,8)
  ,Intensitynu(10000,9)]
Intocloud =7.715E13

Tg=225
c=29979245800.
a= 923.0987/dVd
veen=47966793.28/dVd
;probability of decay into vibrational state for H_2 molecule
p= 0.15
; total oscillator strength of the lyman band
fnl=0.28
; pi*elcharge^2/h*masselectron = con
constant = 1.200789223E35

;calculating H_2 density
for j=0,9 do begin
              NHtwo(*,j) = 5e2
endfor
;calculating H density
for j=0,9 do begin
             Hdensit(*,j) = H-NHtwo(*,j)
endfor
;doing the dissociation part which isn't density dependent
constantc = constant/c
nu = c/lam
```

```
for j=0,9 do begin
               R(*,j)=(p*fnl*constantc*Intensitynu(*,j)*domega(j))
/(nu(*)*2*!pi)
endfor

Rhalf = [R(10000,0), R(10000,1),R(10000,2),R(10000,3),R(10000,4),R(10000,5),
                                    R(10000,6),R(10000,7),R(10000,8),R(10000,9)]
;distance indicator
for i=0,n do begin
        distance(i)=i*Intocloud
endfor
;starting time loop
For z=0,n do begin

        ;first we'll do formation
        ;starting with calculating hydrogen optical depth

        Hdensstep = Hdensit *Intocloud

        for j=0,9 do begin
                NHcolumn(0,j) = Hdensstep(0,j)
        endfor

        for j=0,9 do begin
                FOR i=1,n DO BEGIN
                        NHcolumn(i,j) = NHcolumn(i-1,j) + Hdensstep(i,j)
                ENDFOR
        endfor
        for j=0,9 do begin
                tau(*,j) = 6.3E-18 * NHcolumn(*,j)
        endfor
        Intweeeen(*)=Intensity(*)/1E-21

        Insert(*)=(Intweeeen(*)*domega(*))/(2*!pi)

        for j=0,9 do begin
                Jto(*,j)=8.18E-13*Insert(j)*tau(*,j)^(-2.6666)
        endfor


        for j=0,9 do begin
                Rf(*,j)=1.281E-18*Tg^(1.2979)*Hdensit(*,j)^(1.5)*sqrt(Jto(*,j))
        endfor

        ;Then we'll do dissociation

        NHtwostep=NHtwo*Intocloud


        for j=0,9 do begin
                NHtwocolumn(0,j) = NHtwostep(0,j)
        endfor

        for j=0,9 do begin
                FOR i=1,n DO BEGIN
                        NHtwocolumn(i,j) = NHtwocolumn(i-1,j) + NHtwostep(i,j)
                ENDFOR
```

```
        endfor

        for j=0,9 do begin
                taudis(*,j) = (1.2E-9 * NHtwocolumn(*,j))/dVd
        endfor

        for j=0,9 do begin
                x(*,j)=((taudis(*,j)*a)/(!pi*veen^2))^(0.5)
        endfor

        for j=0,9 do begin
                FOR i=0,n DO if taudis(i,j) LE 1.77 then efc(i,j)=1 ELSE
efc(i,j)=1- ERRORF(x(i,j))
        endfor

        for j=0,9 do begin
                FOR i=0,n DO if taudis(i,j) LE 1.77 then Betaeen(i,j)=0 ELSE
Betaeen(i,j) = 1/(taudis(i,j) * (ALOG(taudis(i,j)/(SQRT(!pi))))^(0.5))
        endfor

        for j=0,9 do begin
                FOR i=0,n DO if taudis(i,j) LE 1.77 then Betatwee(i,j)=1 ELSE
Betatwee(i,j) = (a/taudis(i,j))^(0.5)
        endfor

        for j=0,9 do begin
                Beta(*,j)=(Betaeen(*,j) + Betatwee(*,j))*efc(*,j)
        endfor



        FOR j=0,9 DO BEGIN
                Rd(*,j)= Rhalf(j)* Beta(*,j)
        ENDFOR

        Rdhtwo=Rd * 1.419e10
        Rfhtwo=Rf * 1.419e10
;        time = ((z+1)*(1.419e10))/(31536000.)

        for j=0,9 do begin
                NHtwonew(*,j)=NHtwo(*,j) -Rdhtwo(*,j) +Rfhtwo(*,j)
        endfor

        NHtwonew=(NHtwonew>0)
        for j=0,9 do begin
                Hdensitnew(*,j)=Hdensit(*,j)-NHtwonew(*,j)+NHtwo(*,j)
        endfor

        Hdensit=Hdensitnew
        NHtwo=NHtwonew
        dummy=z
        print,dummy

endfor
for i=0,n do begin
        distance(i)=i*Intocloud
endfor
```

```
;plot,distance,NHtwonew(*,9)
;for i=1,9 do begin
;       oplot,distance,NHtwonew(*,i)
;endfor
for j=0,9 do begin
        openw,1, name(j)
        printf,1,NHtwo(*,j)
        close, 1
endfor
NHtwo3=NHtwo
save,NHtwo3,filename='~/Grootonderzoek/output/NHtwoend410pc.sav'
end
```

Black & van Dishoeck (1987) Abel et al. (1997) Oh & Haiman (2002) Omukai et al. (1999) Demircan & Kahraman (1991) Bromm et al. (2002) Ripamonti et al. (2002) Barkana (2002) Hollenbach & McKee (1979) Abgrall et al. (1992) Abgrall et al. (1993a) Abgrall et al. (1993b) Heger et al. (2002) Baraffe et al. (2001) Bell & Williams (1983) Bertoldi & Draine (1996) Black & Dalgarno (1977) Bromm et al. (2001) Browning et al. (2003) Cayrel (1996) Chabrier & Baraffe (1997) Dalgarno & Stephens (1970) van Dishoeck & Black (1986) Draine & Bertoldi (1996) Draine (1978) Field et al. (1966) Guenther & Demarque (1983) Haiman et al. (2000) Haiman et al. (1997) Haiman et al. (1996) Heger & Woosley (2002) Heger et al. (2002) Henry (2002) Hjellming (1966) Hutchings et al. (2002) Jonin et al. (2000) Kitayama & Ikeuchi (2000) Lee et al. (1996) Marigo et al. (2001) Nakamura & Umemura (1999) Nakamura & Umemura (2002) Norman et al. (2000) Norman & Spaans (1997) Omukai & Nishi (1999) Omukai et al. (1999) Omukai & Palla (2001) Palla et al. (1983) Saumon et al. (1994) Saumon et al. (1995) Schaerer (2002) Scannapieco et al. (2002) Shull (1978) Siess et al. (2002) Spitzer (1947) Stecher & Williams (1967) Suto & Silk (1988) Tumlinson & Shull (2000) Wolniewicz et al. (1998) Yahil (1983) Yan et al. (1998) Zvereva et al. (1982)